Post-print version of:

Publisher: **SAGE**

Journal paper: **Journal of Strain Analysis for Engineering Design 2018, 53(4) 210-224**

Title: **Integral method coefficients for the ring-core technique to evaluate non-uniform residual stresses**

Authors: **M. Barsanti, M. Beghini, C. Santus, A. Benincasa, L. Bertelli**

Integral method coefficients for the ring-core technique to evaluate non-uniform residual stresses

Michele Barsanti[1], Marco Beghini[1], Ciro Santus[1], Alessio Benincasa[2], Lorenzo Bertelli[2]

Abstract

The ring-core technique allows for the determination of non-uniform residual stresses from the surface up to relatively higher depths as compared to the hole-drilling technique. The integral method, which is usually applied to the hole-drilling, can also be used for elaborating the results of the ring-core test since these two experimental techniques share the axisymmetric geometry and the 0-45-90 degrees layout of the strain gage rosette. The aim of this paper is at providing accurate coefficients which can be used for evaluating the residual stress distribution by the ring-core integral method. The coefficients have been obtained by elaborating the results of a very refined plane harmonic axisymmetric finite element model and verified with an independent 3D model. The coefficients for small depth steps were initially provided, then the values for multiple integer step depths were also derived by manipulating the high resolution coefficient matrices, thus showing how the present results can be practically used for obtaining the residual stresses according to different depth sequences, even non-uniform. This analysis also allowed the evaluation of the eccentricity effect which turned out to be negligible due to the symmetry of the problem. An applicative example was reported in which the input of the experimentally measured relaxed strains were elaborated with different depth resolutions, and the obtained residual stress distributions compared.

Keywords

integral method coefficients, depth resolution, eccentricity sensitivity, FE modelling, ring-core.

[1]Dept. of Civil and Industrial Engineering (DICI), University of Pisa, Italy
[2]SINT Technology Srl, Florence, Italy

Corresponding author:
Ciro Santus, University of Pisa, DICI dept. Largo Lucio Lazzarino 1, 56122 Pisa, Italy
Email: ciro.santus@ing.unipi.it

Introduction

The hole-drilling and the ring-core are semi-destructive mechanical techniques used for determining residual stresses at the surface and in the near surface regions, in components with a locally flat surface. Both techniques are based on axisymmetric material removal. The hole-drilling is a well established procedure defined by internationally accepted standards [1;2]. The ring-core was introduced more than 20 years ago [3–6], however it was deeply investigated and developed only recently, especially in terms of sensitivity and uncertainty analysis [7–10], and even applied at the microscale [11;12]. In the hole-drilling the material is removed at the centre of a rosette thus the relaxed strains are measured at the periphery of the hole, whereas in the ring-core the strains are measured in the central internal region, as shown in Figure 1. These two techniques can be considered complementary. The hole-drilling is more popular being dedicated to measure the residual stresses near the surface [13–18] (typically in the layer up to 1 mm, or slightly larger) while the ring-core technique, having a large groove diameter [19], is usually suitable for larger size components where the residual stresses at depths in the order of a few millimetres are of interest, such as rotor forging [20] or thick welded plates [21].
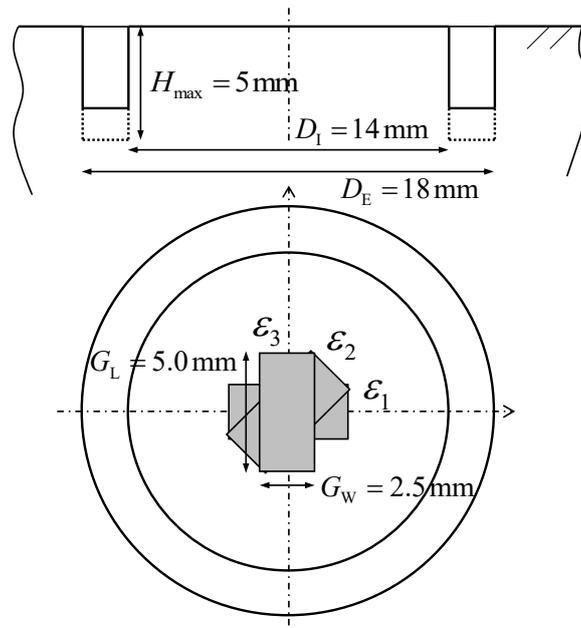
Figure 1. Ring-core technique, typical dimensions of the circular groove and strain gage grids.

Regarding the hole-drilling, the calculation of the residual stresses, after having produced a hole in incremental depths and the relieved strains recorded, can be performed with the standard ASTM E837 – 13a [1] that applies the *integral method*. The same calculation procedure can be applied to elaborate the relaxed strains produced by the ring-core [8;10;22], since the axial-symmetry of the problem and the grid layout according to the 0-45-90 degrees scheme are the same. However, other numerical techniques for the residual stress determination have been proposed, such as the incremental strain method [21;23;24] or the influence function analytical technique as proposed by Beghini et al. [13;14] for the hole-drilling.

This paper presents an accurate Finite Element (FE) analysis, based on the plane harmonic axisymmetric elements, by which the coefficients for applying the integral method to the ring-core were obtained. It is worth noting that the use of a plane model with harmonic elements for solving this problem does not imply any approximation as the element type captures exactly the angular dependence of the solution. This FE approach is highly recommended for a parametric analysis of this type as dramatically reduces the number of nodes and elements if compared to a 3D model with equivalent level of accuracy. Recently, Salvati et al. [12] used an axisymmetric model to interpret the equibiaxial component in a micro ring-core measurement. However, as shown by Barsanti et al. [25] for the hole-drilling method, the axisymmetric elements with the harmonic feature allows to model the shear components too and consequently any in-plane stress condition. In other words, the (simple) axisymmetric element type allows the determination of the equibiaxial matrix $\bar{\mathbf{a}}$, while with the harmonic axisymmetric elements both matrices $\bar{\mathbf{a}}$ and $\bar{\mathbf{b}}$ can be obtained.

The ring-core geometrical parameters are shown in Figure 1 where the grid dimensions reproduce the HBM RY51 rosette. The aim of this paper is to obtain and provide the coefficients for a sequence of small depth steps ($\Delta H = 0.1$ mm) in order to give the possibility to derive, with simple calculations, the coefficients for larger steps too. The consistency of the results was validated with a 3D FE model completely independent from the reference axisymmetric model used for the calculation of the proposed coefficients. Finally, an applicative example illustrates the practical use of the provided coefficients.

Outline of the integral method

For a plane problem under a uniform residual stress field and according to the hypothesis that the grid centre belongs to the cylindrical groove axis, the relationship relating the measured relaxed strain ε_r to the principal (residual) stresses, as introduced by Schajer [26;27], is:

$$\varepsilon_r(\vartheta) = A(\sigma_{max} + \sigma_{min}) + B(\sigma_{max} - \sigma_{min})\cos(2\vartheta) \tag{1}$$

where σ_{max} and σ_{min} are the maximum and minimum residual normal stresses, respectively, ϑ is the angle between the principal direction of σ_{max} and the axis of the grid, and A, B are two constants depending on the geometry and on the elastic material properties E and ν. From equation (1), the following matrix relationship is obtained:

$$\begin{bmatrix} (A+B) & (A-B) & 0 \\ A & A & 2B \\ (A-B) & (A+B) & 0 \end{bmatrix} \begin{bmatrix} \sigma_1 \\ \sigma_3 \\ \tau_{13} \end{bmatrix} = \begin{bmatrix} \varepsilon_1 \\ \varepsilon_2 \\ \varepsilon_3 \end{bmatrix} \tag{2}$$

in which the subscripts 1, 2, 3 are related to the three grid directions according to the 0-45-90 degrees scheme and then 1 and 3 are two orthogonal directions which can be taken as the local reference frame, Figure 1. As the directions 1 and 3 are in general not coincident with the residual stress principal directions, the shear stress component τ_{13} can be nonzero. The form of equation 2 suggests that three scalar relationships can be written in a decoupled form, after introducing three strains and three stresses new variables which are linear combinations of the reference frame strain and stress components. The definitions of these variables

can be retrieved in the standard ASTM E837, and the following quantities are needed to be introduced for the measured strains:

$$p = \frac{\varepsilon_3 + \varepsilon_1}{2} \qquad q = \frac{\varepsilon_3 - \varepsilon_1}{2} \qquad t = \frac{2\varepsilon_2 - (\varepsilon_3 + \varepsilon_1)}{2} = \varepsilon_2 - p \tag{3}$$

in which p is the equibiaxial and q and t are the shear components, and the sign of t is discussed below. The residual stresses can be similarly combined, thus defining an equibiaxial P and two shear components Q, T:

$$P = \frac{\sigma_3 + \sigma_1}{2} \qquad Q = \frac{\sigma_3 - \sigma_1}{2} \qquad T = \tau_{13} \tag{4}$$

After defining the combined strains p, q, t and combined stresses P, Q, T, equation 2 can be rewritten as three decoupled relations:

$$\begin{bmatrix} 2A & 0 & 0 \\ 0 & 2B & 0 \\ 0 & 0 & 2B \end{bmatrix} \begin{bmatrix} P \\ Q \\ T \end{bmatrix} = \begin{bmatrix} p \\ q \\ t \end{bmatrix} \tag{5}$$

By introducing the material Young's modulus and the Poisson's ratio, the relationship available in the ASTM standard [1] can be obtained:

$$-\frac{1}{E} \begin{bmatrix} a(1+v) & 0 & 0 \\ 0 & b & 0 \\ 0 & 0 & b \end{bmatrix} \begin{bmatrix} P \\ Q \\ T \end{bmatrix} = \begin{bmatrix} p \\ q \\ t \end{bmatrix} \tag{6}$$

where the dimensionless positive coefficients a and b only depend on the ratios between the groove diameters and the grid dimensions. In principle, a and b are unaffected by the Poisson's ratio v only for a plane stress model, i.e. for a through-thickness hole geometry, while this is not true in a general three-dimensional problem. The Poisson's ratio dependence in equation (6) is therefore only approximate. In fact, the coefficients are functions of the Poisson's ratio, $a(v)$ and $b(v)$, however in the range $0.25 < v < 0.35$ the differences are in the order of a few percent, thus it is usually assumed: $a = a(0.3)$ and $b = b(0.3)$.

When the residual stresses vary along the depth direction, the same approach can be followed but a vectorial form is required. If the circular groove is performed in n steps, usually each with the same depth ΔH, the scalars p, q, t and P, Q, T are replaced by n-dimensional vectors:

$$\begin{aligned} \mathbf{p} &= (p^{(1)}, p^{(2)}, \ldots, p^{(n)})^{\mathrm{T}} \\ \mathbf{q} &= (q^{(1)}, q^{(2)}, \ldots, q^{(n)})^{\mathrm{T}} \\ \mathbf{t} &= (t^{(1)}, t^{(2)}, \ldots, t^{(n)})^{\mathrm{T}} \end{aligned} \tag{7}$$

and

$$\begin{aligned} \mathbf{P} &= (P^{(1)}, P^{(2)}, \ldots, P^{(n)})^{\mathrm{T}} \\ \mathbf{Q} &= (Q^{(1)}, Q^{(2)}, \ldots, Q^{(n)})^{\mathrm{T}} \\ \mathbf{T} &= (T^{(1)}, T^{(2)}, \ldots, T^{(n)})^{\mathrm{T}} \end{aligned} \tag{8}$$

which represent the combined strains and stresses, respectively, at each i-th depth step: $i = 1, \ldots, n$. The general $p^{(i)}$ term represents the combined relaxed strain (equation 3) measured when the groove depth is $i \times \Delta H$, while $P^{(i)}$ represents the combined stress that is assumed to be uniform from the depth $(i-1) \times \Delta H$ to $i \times \Delta H$. Similar

definitions are valid for $q^{(i)}, t^{(i)}$ and shear stresses $Q^{(i)}, T^{(i)}$. Consequently, the scalars a and b in equation 6 have to be replaced by $n \times n$ lower triangular matrices $\overline{\mathbf{a}}$ and $\overline{\mathbf{b}}$. By combining the definitions and the relations introduced above, the matrix form of the integral method is:

$$-\frac{1+\nu}{E}\overline{\mathbf{a}}\,\mathbf{P} = \mathbf{p} \qquad -\frac{1}{E}\overline{\mathbf{b}}\,\mathbf{Q} = \mathbf{q} \qquad -\frac{1}{E}\overline{\mathbf{b}}\,\mathbf{T} = \mathbf{t} \tag{9}$$

When the matrices $\overline{\mathbf{a}}, \overline{\mathbf{b}}$ are available, the residual stress distribution of any experimental case can be deduced from the measured strains by solving the linear systems 9. The elements a_{ij}, b_{ij} of the just defined calibration matrices for the ring-core are calculated and provided in the next section.

A discussion about the sign of the combined strain t has been already provided by Barsanti et al.[25] for the hole-drilling, and it is reconsidered here for the ring-core as it can be a source of formal errors in the elaboration. After introducing the orientations of the directions 1 and 3, if the second grid is along the bisector of a quadrant where the coordinates have same sign (1st or 3rd quadrant), Figure 2, and the residual shear τ_{13} is positive, a negative (contraction) strain is measured by the second grid after introducing the groove. Assuming no equi-biaxial strain component, the combined strain t is equal to ε_2, equation (3), thus it is negative too. According to equation (9), the combined stress T, that is equal to the shear stress τ_{13}, and the combined strain t have opposite sign, thus confirming the accurate definition of the last of equation (3). On the contrary, if the second grid is aligned with the bisector of a quadrant with opposite sign coordinates (2nd or 4th quadrant) the second grid strain and the shear stress have the same sign, and then the opposite definition of the last of equation (3) is required, in agreement with the ASTM standard. However, the scheme with the second grid along the bisector of the 1st or the 3rd quadrant is preferred in the present work, thus the sign of the last of equations 3 is confirmed.
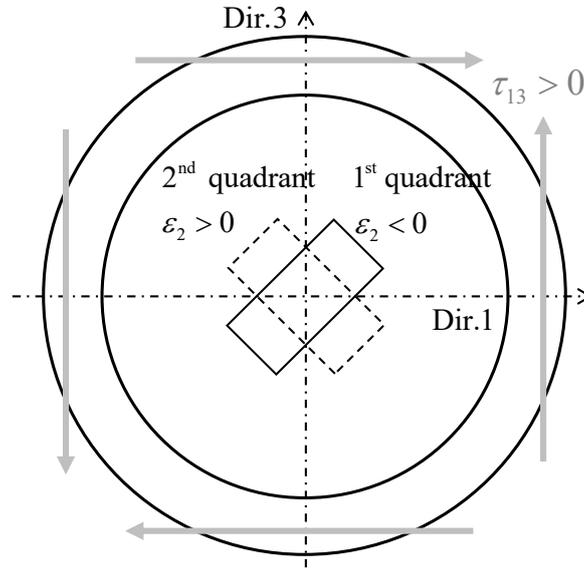
Figure 2. Scheme for deducing the sign of the second grid strain with respect to its angular position.

Axisymmetric harmonic FE model

A refined plane FE model was generated with 5 nested regions having different nodal density. The element size was reduced by a factor of two when passing from one region to the internal one, in order to have the innermost zone, where the material removal is simulated, with 0.1 mm square-shaped elements, and this element edge was 70 times smaller than the internal radius of the groove, Figure 3(a). The FE model height and width were chosen much larger than the groove internal radius, Figure 3(a), to reproduce the condition of a virtually semi-infinite body. The far field boundary conditions influenced the simulated displacements within the groove, and the calculated coefficients, with an estimated effect in the order of 10^{-3}. Approximately 126 000 axisymmetric harmonic elements were used, and the element type was ANSYS® Plane25.

In agreement with equation (9), the general state of residual stress was represented by superimposing an equibiaxial stress and two pure shears. The equibiaxial and the pure shear stress components were applied as two independent load steps, Figure 3(b). Only a single shear stress component was actually required to be modelled, as the matrix to be determined is just $\overline{\mathbf{b}}$ for both shears. The equibiaxial load was modelled with a zero order harmonic analysis, i.e. a radial pressure constant in the angular direction, applied on the cylindrical surfaces of the groove. Whereas, the shear load was obtained by superimposing a normal and a tangential traction distributions, both as second order harmonics with 2ϑ variation, relatively shifted by an angle of $45°$, Figure 3(b).
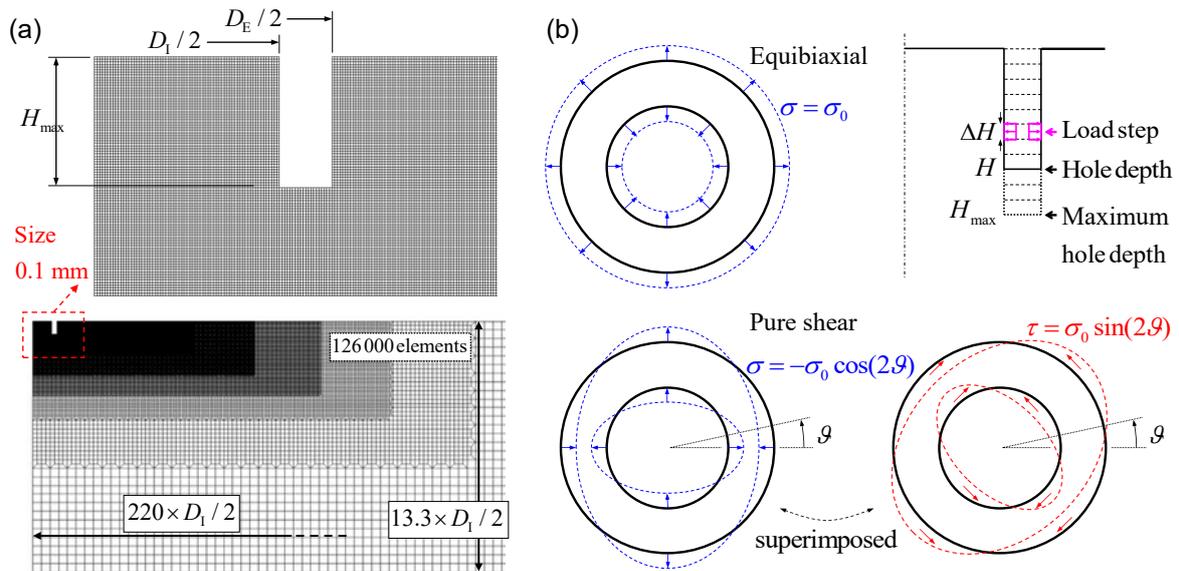
Figure 3. (a) Harmonic plane axisymmetric FE model. (b) Scheme of the basis loading conditions applied to the FE model.

Similarly to the simulations for the hole-drilling technique[25], the FE model is residual stress free, the material at the groove is preliminarily removed and the proper tractions are applied to both the inner and outer cylindrical surfaces. Actually, the physical problem is the opposite. Residual stresses are pre-existing, so the material removal relaxes to zero the tractions at the surfaces of the groove. In order to take into account this

alternative way of modelling, a minus sign has to be introduced in the relation between stresses and strains. In fact, by applying the traction at the free surfaces, the opposite strain is obtained with respect to the theoretical removal of the material.

The same resolution of the model geometry was applied to the integral method load step, thus $\Delta H = 0.1$ mm. For example, when the groove had depth $H = 4.2$ mm, 42 load positions were analysed, the first with the load from 0.0 to 0.1 mm, then from 0.1 to 0.2 mm, and so on. Since the maximum considered groove depth was $H_{\max} = 5.0$ mm, the total number of single simulations (equibiaxial and pure shear) was: $2 \times (50 \times (50 + 1)/2) = 2550$.

Coefficients for the integral method

Coefficient derivation from the displacement fields

The coefficients of the matrices $\overline{\mathbf{a}}, \overline{\mathbf{b}}$ can be derived by imposing a single unitary traction at each depth position, as described in the previous section, and calculating with the FE results the combined strains virtually measured by the rosette. For instance, to calculate the a_{ij} element, the stress components $P^{(j)} = 1$, $P^{(k, k \neq j)} = 0$ were imposed, and the strain component p_i calculated. The simulated strain measured by the grids was evaluated by computing the average displacement (in the grid direction) at the extreme edge segments, and dividing the averaged displacement differences by the grid length, without retrieving any displacement information at the intermediate positions of the grids. With reference to Figure 4, the whole procedure is summarized in detail hereafter:

1. Define the vertices A, B, C, D of each grid and a large enough number of integration points (about 100) on the sides AB and CD, both in cartesian and polar coordinates;

2. Introduce the components of the unit vectors transverse $\hat{\mathbf{t}}$ and normal $\hat{\mathbf{n}}$ (external to the grid) to the segments AB and CD, at each integration point;

3. Calculate the displacements along the radial and the tangential directions by local linear interpolation of the FE element results, at each integration point on sides AB and CD;

4. Evaluate the displacement components along the transverse and normal directions at the integration points;

5. Being the grid mainly sensitive to the extensional strain in the normal direction (transverse sensitivity, though not zero, is quite small and usually neglected) only the displacements along the $\hat{\mathbf{n}}$ direction at the integration points were considered. However, $\hat{\mathbf{t}}$ direction displacements could also be taken into account on the lateral sides BC and AD if the transversal strain sensitivity were significant.

6. Average the normal displacements on the active sides AB and CD.

7. Compute the difference between AB and CD averaged displacements and divide it by the grid length to obtain the simulated measured strains ε_1, ε_3.

8. Evaluate $\varepsilon_1, \varepsilon_3$ to calculate the combined strains p and q, while ε_2 is unnecessary since the shear applied according to the load scheme of Figure 3 (b) is not along the 45 degrees direction.

9. Deduce the matrix coefficients by multiplying p_i by $-E/(1 + \nu)$ for a_{ij}, and q_i by $-E$ for b_{ij}.
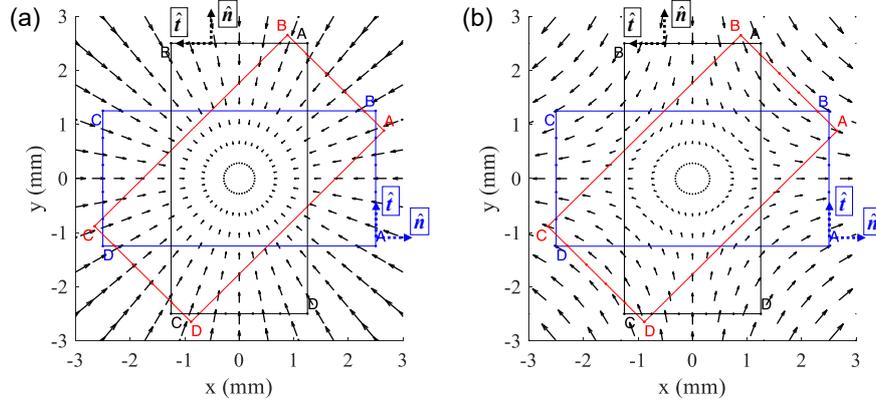
Figure 4. Displacement fields on the strain gage areas: (a) equibiaxial, and (b) pure shear load cases.

This calculation was repeated for all the 2550 simulated groove depths, load depths and load type combinations to obtain the coefficients a_{ij}, b_{ij}, with $i \geq j$ (coefficients with $i < j$ are zero). The $\bar{\mathbf{a}}, \bar{\mathbf{b}}$ matrices obtained for the Poisson's ratio $\nu = 0.3$ are reported in Tables 1 and 2, split in blocks to fit the paper page, and also electronically available on the online Appendix (http://sdj.sagepub.com).

Integer multiple step coefficient determination

Lower resolution coefficients can be derived for any m multiple depth step of $\Delta H = 0.1$ mm, for instance $m = 2, 5, 10$ in order to be applied to measurements with higher depth steps. By implementing the superposition principle, the lower resolution coefficients can be obtained as simple summations of the original coefficients: one every m rows must be taken into account, corresponding to $m \times 0.1$ mm groove depth. For each of these rows, elements must be collected in blocks of size m (starting from the leftmost one), and all the elements in the same block must be summed. At the end of this procedure, two smaller lower triangular matrices of size $(50/m) \times (50/m)$ are obtained.

For example, in order to obtain a_{ij} and b_{ij} for 1 mm depth step ($m = 10$), only the row indices 10, 20, 30, 40, 50 must be considered. In the row with $i = 10$ of the matrix $\bar{\mathbf{a}}$, a single block of 10 values is built, whose sum is 0.1145. In the row with $i = 20$ two blocks of 10 values are built, whose sums are 0.1966 and 0.1139, and so on up to the row with $i = 50$ in which 5 values are obtained by summing the elements contained in each of the 5 blocks. The same procedure is to be repeated for the matrix $\bar{\mathbf{b}}$.

Non-uniform steps, for example as initially proposed by Zuccarello[6], and recently re-proposed by Menda et al.[8;9] and Zuccarello et al.[10], can be also obtained from the large matrices introduced above. However, the depths need to be approximated with the 0.1 mm resolution. At the beginning, the depth 0.6 mm is equivalent to 6 steps of the the high resolution matrices, while 1.05 mm needs to be approximated as 1.1 mm, corresponding to 11 steps. According to this scheme, as graphically shown in Figure 5, the coefficient $a_{11}(b_{11})$ is the sum of all the six elements of the sixth row, then the coefficient $a_{21}(b_{21})$ is the sum of the first six elements of the eleventh row, $a_{22}(b_{22})$ is the sum of the coefficients from the seventh to the eleventh elements, and so on.

Table 1. a_{ij} coefficients ($\times 10^3$) for $D_{\mathrm{I}} = 14$ mm, $D_{\mathrm{E}} = 18$ mm, $G_{\mathrm{L}} = 5.0$ mm, $G_{\mathrm{W}} = 2.5$ mm, maximum depth $H_{\max} = 5.0$ mm and depth resolution $\Delta H = 0.1$ mm.

$$\bar{\mathbf{a}} = \begin{bmatrix} a_1 & \\ a_2 & a_3 \end{bmatrix}$$

a_1

3.8156																								
5.3290	4.5008																							
6.6653	6.0634	5.0409																						
7.9566	7.3646	6.6656	5.4703																					
9.1961	8.6183	7.9611	7.1576	5.8154																				
10.394	9.8140	9.1928	8.4579	7.5586	6.0912																			
11.549	10.967	10.356	9.6764	8.8658	7.8817	6.3073																		
12.661	12.075	11.470	10.814	10.074	9.1941	8.1358	6.4704																	
13.730	13.140	12.537	11.897	11.191	10.393	9.4507	8.3278	6.5856																
14.754	14.160	13.558	12.927	12.245	11.490	10.639	9.6415	8.4633	6.6574															
15.732	15.136	14.534	13.908	13.241	12.517	11.716	10.818	9.7722	8.5471	6.6895														
16.665	16.066	15.463	14.841	14.185	13.482	12.717	11.874	10.934	9.8473	8.5835	6.6855													
17.552	16.951	16.347	15.728	15.080	14.391	13.652	12.849	11.969	10.993	9.8715	8.5765	6.6486												
18.392	17.790	17.186	16.568	15.926	15.249	14.528	13.755	12.918	12.005	10.998	9.8488	8.5299	6.5818											
19.187	18.584	17.979	17.363	16.725	16.057	15.351	14.600	13.795	12.928	11.987	10.955	9.7833	8.4472	6.4882										
19.936	19.332	18.728	18.113	17.479	16.818	16.123	15.389	14.609	13.776	12.884	11.919	10.866	9.6788	8.3319	6.3705									
20.641	20.037	19.432	18.818	18.187	17.532	16.847	16.126	15.365	14.559	13.703	12.788	11.805	10.737	9.5391	8.1874	6.2315								
21.302	20.698	20.094	19.481	18.853	18.202	17.525	16.815	16.070	15.285	14.456	13.579	12.647	11.649	10.571	9.3678	8.0168	6.0737							
21.921	21.317	20.713	20.102	19.476	18.830	18.158	17.458	16.725	15.957	15.151	14.303	13.409	12.463	11.455	10.372	9.1683	7.8233	5.8996						
22.498	21.895	21.292	20.682	20.058	19.415	18.750	18.057	17.335	16.581	15.793	14.968	14.104	13.197	12.242	11.228	10.143	8.9439	7.6097	5.7116					
23.036	22.434	21.832	21.222	20.601	19.961	19.300	18.615	17.901	17.159	16.386	15.580	14.740	13.864	12.948	11.986	10.971	9.8890	8.6980	7.3790	5.5118				
23.536	22.935	22.333	21.726	21.106	20.469	19.813	19.132	18.427	17.694	16.934	16.144	15.323	14.472	13.586	12.664	11.701	10.687	9.6123	8.4336	7.1337	5.3025			
24.000	23.400	22.799	22.193	21.575	20.941	20.288	19.613	18.914	18.190	17.440	16.663	15.859	15.027	14.166	13.275	12.351	11.389	10.381	9.3162	8.1535	6.8763	5.0855		
24.428	23.830	23.230	22.625	22.009	21.378	20.728	20.057	19.364	18.648	17.907	17.141	16.351	15.535	14.695	13.828	12.935	12.012	11.055	10.056	9.0041	7.8605	6.6093	4.8626	
24.824	24.227	23.629	23.025	22.410	21.782	21.135	20.468	19.780	19.070	18.337	17.581	16.802	16.001	15.177	14.331	13.462	12.569	11.650	10.701	9.7138	8.6786	7.5571	6.3349	4.6356

a_2

25.189	24.593	23.996	23.393	22.781	22.154	21.510	20.847	20.164	19.459	18.733	17.985	17.216	16.427	15.617	14.788	13.939	13.071	12.181	11.270	10.331	9.3587	8.3426	7.2459	6.0550
25.524	24.929	24.333	23.733	23.122	22.497	21.856	21.196	20.516	19.817	19.096	18.356	17.596	16.816	16.019	15.204	14.372	13.523	12.658	11.775	10.873	9.9484	8.9932	7.9987	6.9289
25.832	25.238	24.644	24.044	23.435	22.812	22.173	21.516	20.840	20.145	19.430	18.696	17.943	17.173	16.385	15.582	14.765	13.933	13.087	12.228	11.355	10.465	9.5557	8.6200	7.6490
26.113	25.520	24.928	24.329	23.722	23.101	22.464	21.810	21.137	20.446	19.736	19.007	18.261	17.498	16.720	15.927	15.121	14.303	13.474	12.634	11.784	10.922	10.047	9.1555	8.2414
26.370	25.779	25.187	24.590	23.984	23.365	22.730	22.079	21.409	20.721	20.015	19.292	18.551	17.795	17.024	16.241	15.445	14.639	13.824	13.000	12.168	11.328	10.480	9.6217	8.7505
26.604	26.014	25.424	24.828	24.224	23.606	22.973	22.324	21.657	20.973	20.270	19.551	18.816	18.066	17.302	16.526	15.739	14.943	14.139	13.329	12.512	11.691	10.864	10.032	9.1925
26.817	26.229	25.640	25.045	24.442	23.826	23.195	22.548	21.884	21.202	20.503	19.788	19.057	18.312	17.554	16.784	16.005	15.218	14.424	13.625	12.822	12.016	11.206	10.395	9.5804
27.010	26.423	25.835	25.242	24.640	24.026	23.397	22.751	22.089	21.410	20.714	20.002	19.276	18.535	17.782	17.019	16.247	15.467	14.682	13.892	13.100	12.306	11.512	10.717	9.9228
27.186	26.599	26.013	25.421	24.820	24.207	23.579	22.936	22.276	21.599	20.906	20.198	19.474	18.738	17.990	17.232	16.465	15.692	14.914	14.133	13.350	12.567	11.785	11.005	10.226
27.344	26.759	26.173	25.583	24.983	24.371	23.745	23.103	22.445	21.771	21.080	20.374	19.654	18.921	18.177	17.424	16.662	15.895	15.124	14.350	13.575	12.801	12.029	11.261	10.496
27.486	26.903	26.318	25.728	25.130	24.519	23.895	23.254	22.598	21.925	21.237	20.534	19.817	19.087	18.347	17.597	16.840	16.078	15.312	14.545	13.777	13.011	12.248	11.489	10.735
27.615	27.032	26.448	25.860	25.262	24.653	24.029	23.391	22.736	22.065	21.379	20.678	19.963	19.236	18.499	17.753	17.001	16.243	15.482	14.720	13.958	13.199	12.443	11.693	10.949
27.730	27.148	26.565	25.978	25.381	24.773	24.151	23.513	22.860	22.191	21.506	20.807	20.095	19.371	18.637	17.894	17.145	16.391	15.634	14.877	14.121	13.367	12.618	11.875	11.138
27.833	27.252	26.670	26.083	25.488	24.881	24.259	23.623	22.971	22.303	21.621	20.923	20.213	19.491	18.760	18.020	17.274	16.523	15.771	15.018	14.266	13.518	12.774	12.037	11.307
27.924	27.344	26.764	26.178	25.583	24.977	24.357	23.721	23.071	22.404	21.723	21.028	20.319	19.599	18.870	18.133	17.389	16.642	15.893	15.143	14.396	13.652	12.913	12.181	11.458
28.006	27.427	26.847	26.262	25.668	25.062	24.443	23.809	23.159	22.494	21.814	21.120	20.414	19.696	18.969	18.233	17.493	16.748	16.002	15.255	14.511	13.771	13.037	12.310	11.591
28.079	27.500	26.921	26.336	25.743	25.139	24.520	23.887	23.238	22.574	21.896	21.203	20.498	19.782	19.056	18.323	17.584	16.842	16.098	15.355	14.614	13.878	13.147	12.424	11.710
28.143	27.565	26.986	26.403	25.810	25.206	24.589	23.956	23.308	22.646	21.968	21.277	20.573	19.858	19.134	18.403	17.666	16.926	16.185	15.444	14.706	13.972	13.244	12.525	11.814
28.199	27.622	27.044	26.461	25.869	25.266	24.649	24.017	23.370	22.708	22.032	21.341	20.639	19.925	19.203	18.473	17.738	17.000	16.261	15.522	14.786	14.055	13.330	12.614	11.907
28.248	27.672	27.094	26.512	25.921	25.318	24.702	24.071	23.425	22.764	22.088	21.399	20.697	19.985	19.264	18.535	17.802	17.065	16.328	15.591	14.857	14.129	13.406	12.692	11.988
28.292	27.715	27.139	26.557	25.966	25.364	24.748	24.118	23.472	22.812	22.137	21.449	20.748	20.037	19.317	18.590	17.858	17.123	16.387	15.652	14.920	14.193	13.473	12.762	12.060
28.329	27.753	27.177	26.595	26.005	25.404	24.788	24.159	23.514	22.854	22.180	21.492	20.793	20.083	19.364	18.638	17.907	17.173	16.438	15.705	14.975	14.250	13.531	12.822	12.123
28.361	27.786	27.210	26.629	26.039	25.438	24.823	24.194	23.550	22.891	22.217	21.530	20.832	20.122	19.404	18.679	17.949	17.217	16.483	15.751	15.022	14.299	13.582	12.875	12.177
28.389	27.814	27.239	26.658	26.069	25.468	24.853	24.225	23.581	22.922	22.249	21.563	20.865	20.156	19.439	18.715	17.986	17.254	16.522	15.791	15.064	14.342	13.627	12.920	12.224
28.413	27.838	27.263	26.683	26.093	25.493	24.879	24.251	23.607	22.949	22.277	21.591	20.894	20.186	19.469	18.746	18.018	17.287	16.556	15.826	15.099	14.378	13.665	12.960	12.265

a_3

4.4061																								
5.7715	4.1753																							
6.6083	5.4863	3.9446																						
7.2959	6.2859	5.2007	3.7152																					
7.8597	6.9413	5.9634	4.9164	3.4881																				
8.3429	7.4769	6.5870	5.6424	4.6344	3.2642																			
8.7613	7.9348	7.0950	6.2346	5.3243	4.3560	3.0442																		
9.1276	8.3302	7.5282	6.7156	5.8857	5.0102	4.0821	2.8290																	
9.4500	8.6755	7.9012	7.1246	6.3402	5.5414	4.7014	3.8137	2.6191																
9.7349	8.9786	8.2261	7.4760	6.7258	5.9701	5.2030	4.3986	3.5514	2.4149															
9.9874	9.2459	8.5107	7.7813	7.0561	6.3329	5.6066	4.8714	4.1028	3.2959	2.2170														
10.211	9.4821	8.7610	8.0480	7.3424	6.6430	5.9473	5.2507	4.5475	3.8146	3.0478	2.0257													
10.410	9.6913	8.9817	8.2820	7.5919	6.9110	6.2377	5.5700	4.9032	4.2321	3.5347	2.8074	1.8412												
10.587	9.8765	9.1765	8.4878	7.8103	7.1440	6.4881	5.8415	5.2018	4.5649	3.9257	3.2634	2.5751	1.6637											
10.744	10.041	9.3487	8.6690	8.0018	7.3473	6.7052	6.0749	5.4551	4.8436	4.2364	3.6288	3.0013	2.3513	1.4934										
10.883	10.186	9.5008	8.8287	8.1701	7.5252	6.8943	6.2768	5.6722	5.0793	4.4959	3.9182	3.3420	2.7485	2.1360	1.3303									
11.006	10.314	9.6350	8.9694	8.3179	7.6811	7.0592	6.4521	5.8595	5.2809	4.7147	4.1593	3.6109	3.0654	2.5054	1.9295	1.1746								
11.115	10.428	9.7535	9.0932	8.4478	7.8177	7.2032	6.6046	6.0217	5.4542	4.9014	4.3620	3.8342	3.3145	2.7993	2.2720	1.7319	1.0262							
11.211	10.528	9.8577	9.2022	8.5618	7.9373	7.3291	6.7374	6.1624	5.6038	5.0614	4.5343	4.0213	3.5208	3.0295	2.5438	2.0484	1.5430	0.88503						
11.296	10.616	9.9493	9.2977	8.6617	8.0419	7.4389	6.8531	6.2845	5.7332	5.1990	4.6815	4.1799	3.6932	3.2195	2.7559	2.2991	1.8348	1.3629	0.75111					
11.370	10.693	10.030	9.3814	8.7491	8.1334	7.5348	6.9537	6.3905	5.8451	5.3177	4.8078	4.3151	3.8387	3.3777	2.9304	2.4938	2.0652	1.6310	1.1917	0.62427				
11.435	10.760	10.100	9.4545	8.8254	8.2130	7.6187	7.0411	6.4824	5.9419	5.4200	4.9162	4.4305	3.9623	3.5108	3.0750	2.6534	2.2433	1.8361	1.4369	1.0290	0.50445			
11.492	10.819	10.161	9.5182	8.8917	8.2823	7.6905	7.1169	6.5619	6.0256	5.5081	5.0094	4.5292	4.0674	3.6233	3.1962	2.7852	2.3887	2.0042	1.6294	1.2526	0.87490	0.39144		
11.541	10.870	10.214	9.5733	8.9491	8.3422	7.7531	7.1824	6.6305	6.0976	5.5838	5.0892	4.6137	4.1569	3.7186	3.2983	2.8951	2.5082	2.1361	1.7766	1.4274	1.0777	0.72920	0.28509	
11.583	10.914	10.260	9.6209	8.9987	8.3939	7.8071	7.2388	6.6895	6.1595	5.6488	5.1576	4.6857	4.2331	3.7994	3.3843	2.9872	2.6074	2.2439	1.8956	1.5602	1.2357	0.91223	0.59162	0.18524

Validation of the calibration coefficients

A 3D model was implemented for validating the plane FE analysis and the proposed calculation procedure. Though coarser than the axisymmetric model, Figure 6, the load application and the relaxed strain calculation were completely different in this 3D analysis, thus it was unlikely to replicate the same error on both models. The successful comparison, even if verified for a few residual stress cases, gave high confidence about the proper application of the integral method and then the correctness of the coefficients. In principle, the same

Table 2. b_{ij} coefficients ($\times 10^3$) for $D_I = 14$ mm, $D_E = 18$ mm, $G_L = 5.0$ mm, $G_W = 2.5$ mm, maximum depth $H_{max} = 5.0$ mm and depth resolution $\Delta H = 0.1$ mm.

$$\overline{\mathbf{b}} = \begin{bmatrix} b_1 & \\ b_2 & b_3 \end{bmatrix}$$

b_1

5.2582																								
6.7987	5.9027																							
8.2099	7.5041	6.4355																						
9.6160	8.8915	8.1143	6.8750																					
11.007	10.277	9.5120	8.6368	7.2450																				
12.396	11.644	10.894	10.059	9.0867	7.5592																			
13.784	13.009	12.248	11.449	10.538	9.4742	7.8252																		
15.171	14.373	13.597	12.799	11.941	10.954	9.8063	8.0481																	
16.558	15.736	14.940	14.137	13.291	12.370	11.312	10.087	8.2314																
17.944	17.097	16.280	15.464	14.621	13.722	12.741	11.616	10.321	8.3776															
19.327	18.456	17.617	16.785	15.935	15.046	14.093	13.054	11.868	10.509	8.4888														
20.706	19.810	18.948	18.098	17.237	16.347	15.411	14.407	13.313	12.071	10.655	8.5666													
22.078	21.158	20.273	19.403	18.528	17.632	16.700	15.717	14.663	13.520	12.226	10.760	8.6126												
23.443	22.499	21.590	20.699	19.807	18.901	17.967	16.992	15.964	14.865	13.675	12.336	10.826	8.6285											
24.799	23.830	22.897	21.984	21.074	20.155	19.213	18.240	17.224	16.154	15.012	13.782	12.403	10.854	8.6157										
26.142	25.148	24.192	23.256	22.327	21.393	20.441	19.464	18.453	17.398	16.288	15.109	13.842	12.428	10.847	8.5758									
27.471	26.453	25.473	24.515	23.566	22.614	21.651	20.666	19.654	18.606	17.514	16.369	15.155	13.857	12.413	10.807	8.5104								
28.785	27.742	26.738	25.757	24.788	23.818	22.840	21.846	20.828	19.781	18.699	17.574	16.397	15.154	13.829	12.361	10.735	8.4210							
30.080	29.013	27.985	26.981	25.991	25.003	24.010	23.003	21.978	20.928	19.849	18.736	17.581	16.376	15.108	13.761	12.274	10.633	8.3094						
31.356	30.264	29.212	28.186	27.175	26.168	25.158	24.138	23.102	22.047	20.968	19.859	18.718	17.537	16.309	15.020	13.654	12.154	10.504	8.1771					
32.610	31.494	30.418	29.370	28.337	27.311	26.284	25.249	24.202	23.139	22.055	20.948	19.813	18.647	17.444	16.196	14.891	13.512	12.003	10.349	8.0259				
33.840	32.700	31.601	30.530	29.476	28.431	27.386	26.336	25.277	24.203	23.114	22.004	20.872	19.714	18.527	17.305	16.042	14.724	13.338	11.824	10.170	7.8875			
35.046	33.882	32.760	31.667	30.592	29.527	28.464	27.398	26.325	25.241	24.143	23.028	21.895	20.741	19.564	18.359	17.123	15.849	14.523	13.132	11.619	9.9701	7.6736		
36.226	35.038	33.893	32.778	31.682	30.597	29.516	28.435	27.347	26.251	25.144	24.023	22.886	21.733	20.560	19.366	18.148	16.902	15.620	14.290	12.899	11.390	9.7507	7.4757	
37.378	36.167	34.999	33.862	32.745	31.641	30.543	29.444	28.343	27.234	26.116	24.987	23.845	22.689	21.519	20.331	19.125	17.897	16.643	15.358	14.028	12.640	11.139	9.5140	7.2656

b_2

38.501	37.267	36.077	34.919	33.782	32.658	31.542	30.427	29.310	28.189	27.060	25.921	24.773	23.613	22.441	21.256	20.057	18.842	17.608	16.351	15.065	13.739	12.359	10.870	9.2620
39.595	38.338	37.126	35.947	34.790	33.647	32.513	31.382	30.250	29.115	27.974	26.826	25.670	24.505	23.330	22.146	20.950	19.742	18.521	17.285	16.028	14.746	13.426	12.057	10.583
40.659	39.379	38.146	36.946	35.769	34.608	33.456	32.309	31.162	30.013	28.861	27.702	26.538	25.366	24.187	23.000	21.805	20.602	19.390	18.167	16.930	15.678	14.402	13.093	11.737
41.691	40.390	39.136	37.915	36.719	35.540	34.370	33.207	32.045	30.883	29.718	28.549	27.375	26.196	25.011	23.821	22.626	21.424	20.217	19.003	17.781	16.549	15.303	14.037	12.741
42.692	41.370	40.095	38.854	37.639	36.442	35.256	34.076	32.900	31.724	30.546	29.367	28.183	26.996	25.805	24.611	23.412	22.211	21.006	19.798	18.585	17.368	16.142	14.906	13.653
43.661	42.318	41.023	39.763	38.530	37.314	36.112	34.916	33.725	32.536	31.346	30.155	28.962	27.767	26.569	25.369	24.167	22.964	21.760	20.555	19.349	18.141	16.930	15.715	14.491
44.598	43.234	41.919	40.641	39.390	38.157	36.938	35.728	34.522	33.319	32.118	30.915	29.712	28.508	27.303	26.097	24.891	23.685	22.480	21.276	20.074	18.872	17.672	16.472	15.269
45.503	44.119	42.785	41.488	40.219	38.970	37.735	36.510	35.290	34.074	32.860	31.647	30.434	29.221	28.008	26.796	25.585	24.375	23.168	21.964	20.763	19.566	18.373	17.183	15.995
46.375	44.972	43.620	42.305	41.019	39.754	38.503	37.263	36.030	34.801	33.575	32.351	31.128	29.906	28.685	27.466	26.249	25.036	23.826	22.620	21.420	20.225	19.037	17.854	16.676
47.216	45.794	44.423	43.091	41.789	40.507	39.242	37.987	36.741	35.500	34.262	33.027	31.794	30.563	29.335	28.109	26.886	25.667	24.454	23.246	22.045	20.851	19.665	18.488	17.318
48.024	46.584	45.196	43.847	42.528	41.232	39.952	38.684	37.424	36.171	34.922	33.676	32.433	31.194	29.957	28.724	27.495	26.271	25.054	23.843	22.641	21.447	20.262	19.087	17.922
48.801	47.343	45.938	44.573	43.239	41.928	40.633	39.352	38.080	36.814	35.554	34.298	33.046	31.797	30.553	29.312	28.077	26.849	25.627	24.413	23.208	22.013	20.828	19.655	18.494
49.547	48.072	46.650	45.270	43.921	42.595	41.287	39.992	38.708	37.431	36.160	34.894	33.632	32.375	31.123	29.875	28.634	27.400	26.173	24.955	23.748	22.551	21.366	20.193	19.034
50.262	48.770	47.333	45.938	44.574	43.234	41.913	40.606	39.310	38.021	36.740	35.464	34.193	32.928	31.667	30.413	29.166	27.926	26.694	25.473	24.262	23.063	21.876	20.704	19.545
50.947	49.434	47.987	46.577	45.199	43.846	42.512	41.193	39.885	38.586	37.295	36.009	34.730	33.456	32.188	30.927	29.673	28.427	27.191	25.965	24.751	23.549	22.361	21.188	20.029
51.603	50.079	48.612	47.188	45.797	44.431	43.085	41.754	40.435	39.126	37.824	36.530	35.242	33.960	32.684	31.416	30.156	28.905	27.664	26.434	25.216	24.012	22.821	21.647	20.488
52.229	50.691	49.210	47.772	46.368	44.990	43.632	42.290	40.960	39.641	38.330	37.027	35.730	34.440	33.158	31.883	30.617	29.361	28.115	26.880	25.659	24.451	23.258	22.082	20.922
52.828	51.276	49.781	48.330	46.913	45.523	44.154	42.801	41.462	40.132	38.812	37.500	36.196	34.898	33.609	32.328	31.056	29.794	28.543	27.304	26.079	24.868	23.673	22.495	21.334
53.399	51.833	50.325	48.862	47.433	46.032	44.652	43.289	41.939	40.601	39.272	37.951	36.639	35.335	34.038	32.751	31.473	30.206	28.950	27.707	26.478	25.264	24.066	22.886	21.723
53.944	52.365	50.844	49.369	47.929	46.516	45.126	43.753	42.394	41.046	39.709	38.381	37.061	35.749	34.447	33.153	31.870	30.598	29.337	28.090	26.857	25.640	24.439	23.256	22.092
54.462	52.871	51.338	49.851	48.400	46.977	45.577	44.194	42.826	41.470	40.125	38.789	37.462	36.144	34.835	33.536	32.247	30.970	29.705	28.454	27.217	25.996	24.793	23.607	22.441
54.956	53.352	51.808	50.310	48.849	47.416	46.006	44.614	43.238	41.874	40.520	39.177	37.843	36.519	35.204	33.899	32.605	31.323	30.054	28.798	27.558	26.334	25.128	23.940	22.771
55.426	53.810	52.255	50.747	49.275	47.833	46.414	45.013	43.628	42.257	40.896	39.546	38.205	36.874	35.554	34.243	32.944	31.658	30.384	29.125	27.881	26.654	25.445	24.254	23.084
55.872	54.246	52.680	51.162	49.680	48.229	46.801	45.392	43.999	42.620	41.252	39.895	38.549	37.212	35.886	34.570	33.266	31.975	30.697	29.434	28.187	26.957	25.745	24.552	23.379
56.296	54.659	53.083	51.555	50.065	48.604	47.168	45.751	44.351	42.965	41.590	40.227	38.874	37.532	36.200	34.880	33.571	32.276	30.994	29.727	28.477	27.244	26.029	24.834	23.659

b_3

7.0449																								
8.9966	6.8150																							
10.282	8.7196	6.5774																						
11.402	9.9687	8.4330	6.3336																					
12.373	11.054	9.6445	8.1384	6.0849																				
13.254	11.992	10.695	9.3117	7.8374	5.8326																			
14.060	12.840	11.600	10.326	8.9720	7.5317	5.5777																		
14.807	13.616	12.416	11.198	9.9512	8.6273	7.2226	5.3216																	
15.503	14.333	13.161	11.983	10.790	9.5709	8.2790	6.9116	5.0651																
16.155	14.999	13.848	12.698	11.544	10.377	9.1872	7.9288	6.5998	4.8092															
16.768	15.623	14.486	13.356	12.229	11.100	9.9612	8.8017	7.5779	6.2884	4.5547														
17.344	16.207	15.081	13.965	12.858	11.755	10.654	9.5437	8.4159	7.2277	5.9785	4.3026													
17.888	16.757	15.638	14.533	13.440	12.357	11.280	10.206	9.1264	8.0312	6.8794	5.6710	4.0534												
18.402	17.274	16.161	15.064	13.981	12.912	11.854	10.805	9.7599	8.7107	7.6487	6.5338	5.3669	3.8078											
18.887	17.762	16.653	15.561	14.486	13.427	12.383	11.352	10.331	9.3155	8.2979	7.2697	6.1922	5.0668	3.5664										
19.346	18.222	17.116	16.029	14.959	13.908	12.873	11.855	10.852	9.8595	8.8746	7.8890	6.8951	5.8552	4.7715	3.3296									
19.780	18.657	17.553	16.468	15.402	14.357	13.330	12.322	11.331	10.355	9.3925	8.4384	7.4854	6.5258	5.5236	4.4816	3.0980								
20.191	19.068	17.964	16.881	15.819	14.777	13.756	12.755	11.774	10.811	9.8640	8.9311	8.0081	7.0877	6.1627	5.1981	4.1977	2.8717							
20.580	19.456	18.353	17.271	16.210	15.172	14.155	13.159	12.185	11.231	10.296	9.3787	8.4762	7.5845	6.6969	5.8064	4.8794	3.9201	2.6514						
20.947	19.823	18.719	17.638	16.579	15.542	14.528	13.537	12.568	11.621	10.695	9.7886	8.9009	8.0286	7.1685	6.3136	5.4575	4.5678	3.6493	2.4370					
21.295	20.169	19.066	17.984	16.926	15.890	14.878	13.890	12.925	11.983	11.064	10.166	9.2891	8.4312	7.5895	6.7609	5.9386	5.1166	4.2639	3.3856	2.2289				
21.623	20.497	19.392	18.311	17.252	16.218	15.209	14.221	13.259	12.321	11.406	10.515	9.6464	8.7987	7.9705	7.1594	6.3621	5.5723	4.7841	3.9679	3.1294	2.0273			
21.934	20.806	19.701	18.619	17.560	16.526	15.516	14.531	13.571	12.636	11.725	10.839	9.9763	9.1364	8.3181	7.5198	6.7391	5.9729	5.2151	4.4605	3.6802	2.8808	1.8323		
22.228	21.099	19.992	18.909	17.850	16.816	15.807	14.823	13.864	12.931	12.023	11.140	10.282	9.4481	8.6370	7.8481	7.0794	6.3290	5.5936	4.8676	4.1459	3.4011	2.6399	1.6439	
22.505	21.375	20.267	19.183	18.123	17.089	16.080	15.096	14.139	13.207	12.301	11.421	10.566	9.7366	8.9311	8.1490	7.3891	6.6501	5.9295	5.2246	4.5300	3.8407	3.1306	2.4070	1.4623

level of accuracy would have been obtained with a 3D model just by replicating the discretization in the section plane and then introducing a large number of divisions, for example 100, along the angular direction. However, such a higher number of elements would require huge computing performances, basically without any significant advantage.

In the 3D analyses, the external load was applied as far field along the two principal directions *x* and *y* and the material removal simulated with no traction applied to the groove surfaces. The relaxed strains were then

$a_{ij} \, (\times 10^3)$

(a)

3.8156										
5.3290	4.5008									
6.6653	6.0634	5.0409								
7.9566	7.3646	6.6656	5.4703							
9.1961	8.6183	7.9611	7.1576	5.8154						
10.394	9.8140	9.1928	8.4579	7.5586	6.0912					
11.549	10.967	10.356	9.6764	8.8658	7.8817	6.3073				
12.661	12.075	11.470	10.814	10.074	9.1941	8.1358	6.4704			
13.730	13.140	12.537	11.897	11.191	10.393	9.4507	8.3278	6.5856		
14.754	14.160	13.558	12.927	12.245	11.490	10.639	9.6415	8.4633	6.6574	
15.732	15.136	14.534	13.908	13.241	12.517	11.716	10.818	9.7722	8.5471	6.6895

6 steps → 11 steps →

$\sum_{j=1}^{6} a_{6j}$ $\sum_{j=1}^{6} a_{11j}$ $\sum_{j=7}^{11} a_{11j}$

$b_{ij} \, (\times 10^3)$

(b)

5.2582										
6.7987	5.9027									
8.2099	7.5041	6.4355								
9.6160	8.8915	8.1143	6.8750							
11.007	10.277	9.5120	8.6368	7.2450						
12.396	11.644	10.894	10.059	9.0867	7.5592					
13.784	13.009	12.248	11.449	10.538	9.4742	7.8252				
15.171	14.373	13.597	12.799	11.941	10.954	9.8063	8.0481			
16.558	15.736	14.940	14.137	13.291	12.370	11.312	10.087	8.2314		
17.944	17.097	16.280	15.464	14.621	13.722	12.741	11.616	10.321	8.3776	
19.327	18.456	17.617	16.785	15.935	15.046	14.093	13.054	11.868	10.509	8.4888

6 steps → 11 steps →

$\sum_{j=1}^{6} b_{6j}$ $\sum_{j=1}^{6} b_{11j}$ $\sum_{j=7}^{11} b_{11j}$

Figure 5. Calculation scheme with non-uniform depths for deriving the lower resolution coefficients of matrices a_{ij} (a) and b_{ij} (b).

(a) σ_y

σ_x

Grid 1 angle ϑ

(b) 510 000 elements

Grid side points

Outside point by symmetry

Symmetry

Figure 6. FE model for validation, (a) load scheme, (b) 3D mesh grid side points.

obtained as the difference between the final grooved geometry and the load uniformly applied before the material removal, which could be computed with the Hooke's law. The problem features two symmetry planes which were considered to reduce the modelled volume by a factor of 4. The grid side points were simulated as any angle with respect to the first principal direction x and those points outside the quarter volume were computed by exploiting the symmetries of the problem. The matrices for the integral method according to 0.5

mm resolution of the 3D model, were obtained by applying the procedure introduced in the previous section, and reported in Table 3. Equations (9) were inverted to obtain the stresses, assuming as input the strains of the 3D FE analysis which was treated as a virtual residual stress experiment.

Table 3. Calibration coefficients with resolution $\Delta H = 0.5$ mm for the validation analysis.

a_{ij} coefficients ($\times 10^3$)									
38.75	0	0	0	0	0	0	0	0	0
67.64	46.89	0	0	0	0	0	0	0	0
89.84	72.73	47.66	0	0	0	0	0	0	0
106.4	90.14	70.30	43.64	0	0	0	0	0	0
118.1	102.2	83.90	62.71	36.92	0	0	0	0	0
125.9	110.3	92.68	73.15	52.35	29.17	0	0	0	0
130.8	115.4	98.21	79.45	60.16	41.14	21.54	0	0	0
133.8	118.5	101.5	83.20	64.60	46.80	30.43	14.71	0	0
135.4	120.3	103.4	85.32	67.07	49.82	34.35	20.97	9.004	0
136.3	121.2	104.4	86.43	68.37	51.38	36.29	23.52	13.12	4.485
b_{ij} coefficients ($\times 10^3$)									
46.68	0	0	0	0	0	0	0	0	0
81.41	56.78	0	0	0	0	0	0	0	0
114.6	90.99	60.67	0	0	0	0	0	0	0
146.2	120.6	93.39	59.51	0	0	0	0	0	0
175.2	147.2	119.2	89.35	54.59	0	0	0	0	0
200.7	170.4	140.9	111.0	80.65	47.29	0	0	0	0
222.3	190.0	159.0	128.4	98.37	69.24	38.90	0	0	0
240.1	206.0	173.7	142.2	111.9	83.35	56.81	30.39	0	0
254.4	218.8	185.3	153.0	122.3	93.71	67.79	44.58	22.43	0
265.7	228.8	194.4	161.4	130.2	101.5	75.61	52.96	33.34	15.37

The calculated stress components were finally compared with the stresses imposed to the 3D model, after applying a tensor rotation to obtain the components according to the 1, 3 grid rosette frame. Indeed, a misalignment angle was introduced between the principal stress directions and the rosette frame to have a nonzero shear stress τ_{13} which also allowed to verify the sign definition of the strain component t (equation 3). Five load and angle combinations were considered and the average stress over the depth of 5 mm of each component was compared to the reference value, then the differences were evaluated. This comparison is shown in Table 4 in which differences not larger than 1% are shown, and in Figure 7 where the three stress components of the last case of Table 4 are plotted. The back-calculated stress distributions resulted quite uniform with just small variations at the extremes where the method is more sensitive to the disturbance, and the slight different results of the two FE models produced a detectable effect. It is worth noting that these differences are mainly to be imputed to the coarseness of the 3D analysis, as the plane axisymmetric model features a finer mesh and an exact angular dependence.

Table 4. Validation cases with different combinations of loads and rosette angles, and obtained small average stress differences.

σ_x, MPa	σ_y, MPa	σ_y/σ_x	Grid 1 ϑ	σ_1 diff.	σ_3 diff.	τ_{13} diff.
100	0	0.0	0°	0.1%	–	–
100	100	1.0	0°	−0.2%	−0.2%	–
100	−100	−1.0	0°	0.3%	0.3%	–
75	−30	−0.4	−45°	−0.2%	−0.2%	0.3%
75	−30	−0.4	20°	0.2%	1.0%	0.3%
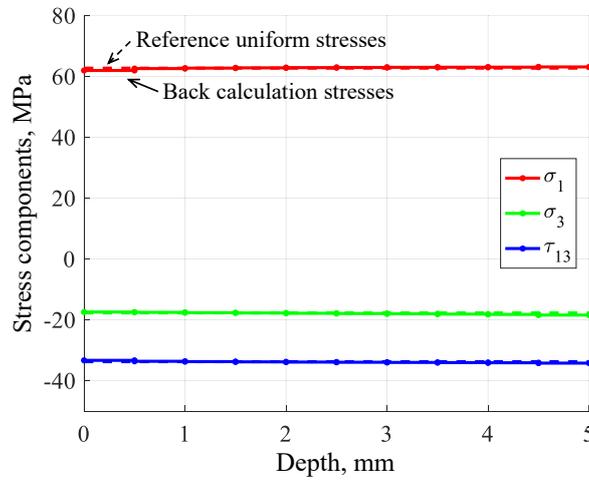
Figure 7. Comparison between the imposed and the back-calculated stresses of a validation case.

Sensitivity to eccentricity

The eccentricity between the hole and the rosette is an important issue in the hole-drilling method. The generalization of the integral method proposed by Barsanti et al. [25], for taking into account of the eccentricity in the hole-drilling, was adapted to the ring-core too. According to that general approach, the p, q, t and P, Q, T decomposition can be no more applied as the axisymmetry of the problem is lost. A more general (still linear) relationship between all the components of stress and strain is consequently introduced:

$$-\frac{1}{E}\overline{\mathbf{A}}\mathbf{S} = \mathbf{e} \tag{10}$$

In equation (10), $\mathbf{S} = (\sigma_1^{(1)}, \sigma_3^{(1)}, \tau_{13}^{(1)}, \ldots, \sigma_1^{(n)}, \sigma_3^{(n)}, \tau_{13}^{(n)})^{\mathrm{T}}$ is the vector collecting all the components of residual stresses in blocks of three elements (one block for each drilling depth) and $\mathbf{e} = (\varepsilon_1^{(1)}, \varepsilon_2^{(1)}, \varepsilon_3^{(1)}, \ldots, \varepsilon_1^{(n)}, \varepsilon_2^{(n)}, \varepsilon_3^{(n)})^{\mathrm{T}}$ is the vector collecting the relaxed strains, again in blocks of three

elements. The lower triangular 3×3 block matrix $\overline{A}$ is defined in equation (11):

$$\overline{\mathbf{A}} = \begin{bmatrix} A_{11}^{(11)} & A_{12}^{(11)} & A_{13}^{(11)} & 0 & 0 & 0 & 0 & 0 & 0 \\ A_{21}^{(11)} & A_{22}^{(11)} & A_{23}^{(11)} & 0 & 0 & 0 & 0 & 0 & 0 \\ A_{31}^{(11)} & A_{32}^{(11)} & A_{33}^{(11)} & 0 & 0 & 0 & 0 & 0 & 0 \\ A_{11}^{(21)} & A_{12}^{(21)} & A_{13}^{(21)} & A_{11}^{(22)} & A_{12}^{(22)} & A_{13}^{(22)} & 0 & 0 & 0 \\ A_{21}^{(21)} & A_{22}^{(21)} & A_{23}^{(21)} & A_{21}^{(22)} & A_{22}^{(22)} & A_{23}^{(22)} & 0 & 0 & 0 \\ A_{31}^{(21)} & A_{32}^{(21)} & A_{23}^{(21)} & A_{31}^{(22)} & A_{32}^{(22)} & A_{33}^{(22)} & 0 & 0 & 0 \\ A_{11}^{(31)} & A_{12}^{(31)} & A_{13}^{(31)} & A_{11}^{(32)} & A_{12}^{(32)} & A_{13}^{(32)} & A_{11}^{(33)} & A_{12}^{(33)} & A_{13}^{(33)} \\ A_{21}^{(31)} & A_{22}^{(31)} & A_{23}^{(31)} & A_{21}^{(32)} & A_{22}^{(32)} & A_{23}^{(32)} & A_{21}^{(33)} & A_{22}^{(33)} & A_{23}^{(33)} \\ A_{31}^{(31)} & A_{32}^{(31)} & A_{33}^{(31)} & A_{31}^{(32)} & A_{32}^{(32)} & A_{33}^{(32)} & A_{31}^{(33)} & A_{32}^{(33)} & A_{33}^{(33)} \end{bmatrix} \tag{11}$$

The elements $A_{hk}^{(ij)}$ have indices $h, k = 1, \ldots, 3$, $i = 1, \ldots, n$ and $j = 1, \ldots, i$, where n is the number of drilling steps. Each coefficient of this matrix depends on the eccentricity components e_1 and e_3 defined in the frame of the grid with axes in the directions 1 and 3 as shown in Figure 8. A power series expansion can be used to represent the dependence of these coefficients to the eccentricity, as shown in equation (12):

$$A_{hk}^{(ij)} = A_{0,hk}^{(ij)} + \frac{\partial A_{hk}^{(ij)}}{\partial e_1} e_1 + \frac{\partial A_{hk}^{(ij)}}{\partial e_3} e_3 + \frac{1}{2} \frac{\partial^2 A_{hk}^{(ij)}}{\partial e_1^2} e_1^2 + \frac{1}{2} \frac{\partial^2 A_{hk}^{(ij)}}{\partial e_3^2} e_3^2 + \frac{\partial^2 A_{hk}^{(ij)}}{\partial e_1 \partial e_3} e_1 e_3 + \ldots. \tag{12}$$

If the eccentricity is small, as it is expected in a correctly applied procedure, only the constant and the linear terms of these expansions are sufficient to approximate the effect. For the hole-drilling, both the two first order derivatives are nonzero, while these terms are zero for the ring core. The physical reason of this result is the symmetry property of the geometry. As the grids are located at the centre, a displacement of the groove either parallel or orthogonal with respect to the grid direction, produces a higher sensitivity at one side and a lower sensitivity at the opposite side, as schematically shown in Figure 8, thus inducing a compensating effect. In fact, a displacement of the grid along a direction produces the same layout as the opposite direction plus a rotation of 180 degrees, which this latter is equivalent from the stress point of view. On the contrary for the hole-drilling technique, a first order net effect results unless special compensating grids are used, as investigated by Beghini et al.[28] and used by Iurea et al.[29], featuring an opposite grid, connected in series, for each of the three directions.

Numerical evaluation of the elements $A_{hk}^{(ij)}$ for different eccentricities performed with the proposed model, numerically confirmed that the ring-core method does not experience sensitivity to eccentricity at the first order. Two examples of this analysis are reported in Figure 9 in which it is evident that the tangent plane of the functions $A_{hk}^{(ij)}(e_1, e_3)$ at the origin is horizontal, with typical local shapes which are either an ellipsoidal surface, Figure 9(a), or a saddle surface, Figure 9(b). For this reason, it was considered not necessary to introduce the form of equation (10) which is more cumbersome, and then the procedure based on p, q, t was assumed accurate enough even with a moderate eccentricity. Indeed, as evident in Figure 9 for the examined geometry, the coefficients $A_{hk}^{(ij)}$ vary less than 1% when the eccentricity vector components (e_1, e_3) are in the

range ± 0.2 mm. The effects of the second order terms in equation 12 are significant only for eccentricities which are relatively large and uncommon in typical experimental applications.

Hole drilling as reference   Ring core
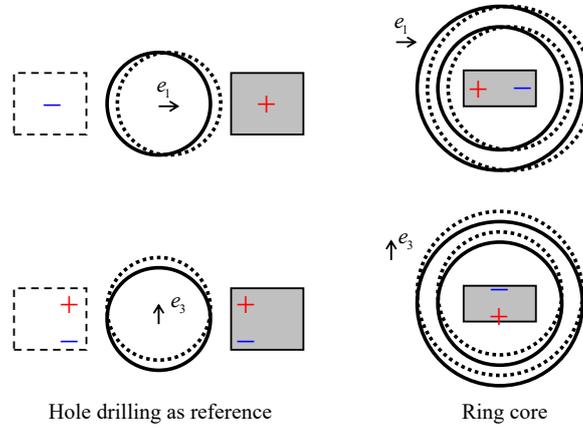
Figure 8. Self compensated eccentricity sensitivity of the ring-core, comparison with the hole-drilling.
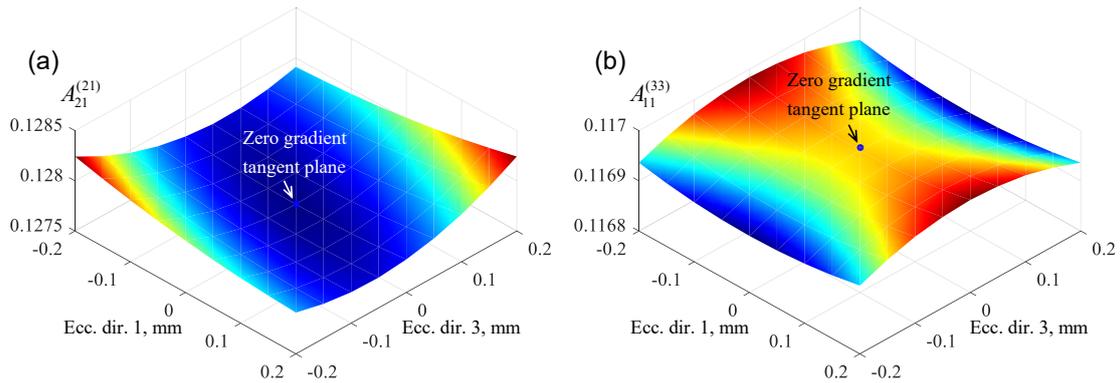
Figure 9. Eccentricity sensitivity of the general form matrix coefficients: (a) A_{21}^{21}, (b) A_{11}^{33} examples, and zero first partial derivatives at the origin.

Experimental application

The mechanical system for automatically drilling the groove and performing the strain gage measurement, manufactured by SINT Technology[30], is shown in Figure 10 along with the HBM RY51 rosette. The drilling spindle of the device is hollow thus allowing the strain gage cables to pass through. The rosette requires a special preparation to protect the grids during the drilling. The overall dimensions of the system are 310 mm long, 160 mm wide, 230 mm maximum height. The centring is performed with two independent mechanical micrometric guides and a control webcam, connected with Ethernet TCP/IP. By this system a positioning accuracy in the order of ± 0.15 mm can be obtained. The vertical feed motion is driven by a stepping motor, and the machining of the annular groove around the strain gage rosette is operated with a DC motor to have

the tool rotational speed at approximately 200 rpm.
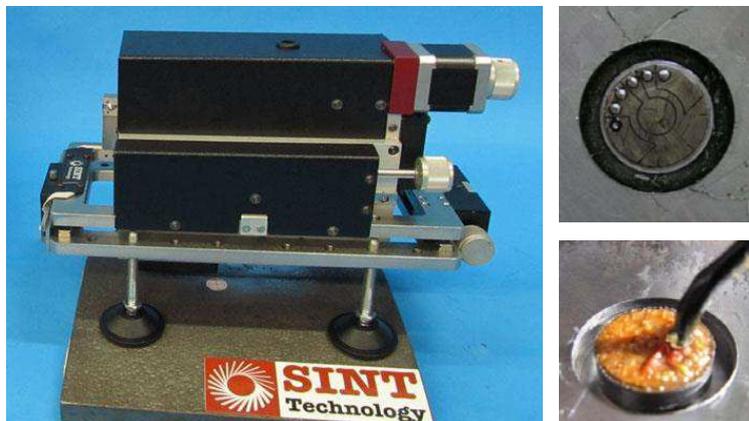
Figure 10. Equipment by SINT Technology for the ring-core automatic testing and HBM rosette.

The application introduced here is not intended to represent a validation, but an experimental example in which the residual stresses are effectively evaluated with different resolutions by means of the proposed coefficients. The ring-core rosette was applied on the lateral surface of a tubular square bar made by ASTM A500 Grade B steel carrying a longitudinal weld. The centre of the measurement region was at 40 mm from the weld, and the grid 1 direction perpendicular to the weld bead. The measured relaxed strains with 0.1 mm milling tool incremental step are plotted in Figure 11 (a). Initially, the residual stresses were calculated with two resolutions, Figure 11 (b): 1.0 mm (dashed lines) and 0.5 mm (solid lines). Higher resolution residual stress distributions, such as 0.2 mm or even 0.1 mm, can also be calculated with the proposed calibration matrices. However, for these small step values, the application of a filtering technique when solving equations 9 is recommended to reduce the effect of the noise. In particular the Tikhonov regularization proposed in the standard ASTM E837, which can be applied to the integral method for the ring core in the same way as for the hole-drilling, was demonstrated by Barsanti et al.[31] to mitigate the effect of the measurement noise. Finally, the non-uniform step sequence, proposed by Zuccarello[6] for this arrangement, with 8 depth increments and optimized strain measurement sensitivity, was implemented by means of the coefficients derived with the calculation scheme of Figure 5. The obtained residual stress distribution is reported in Figure 11 (c), where it is evident that the trends of the components are quite similar to the solution obtained with 0.5 mm step. In fact, the optimized step sizes range between 0.4 mm and 0.7 mm up to 3.5 mm depth.

Conclusions

The paper provides the calibration coefficients to apply the integral method in the ring-core technique for measuring non-uniform in depth residual stress distributions. The harmonic plane axisymmetric finite element model used for the numerical simulation was described along with the procedure to deduce the numerically simulated measured strains. The use of a 2D FE model produced results with high resolution and accuracy. Similar results could be obtained with a more intuitive 3D model but with 2 orders of magnitude more
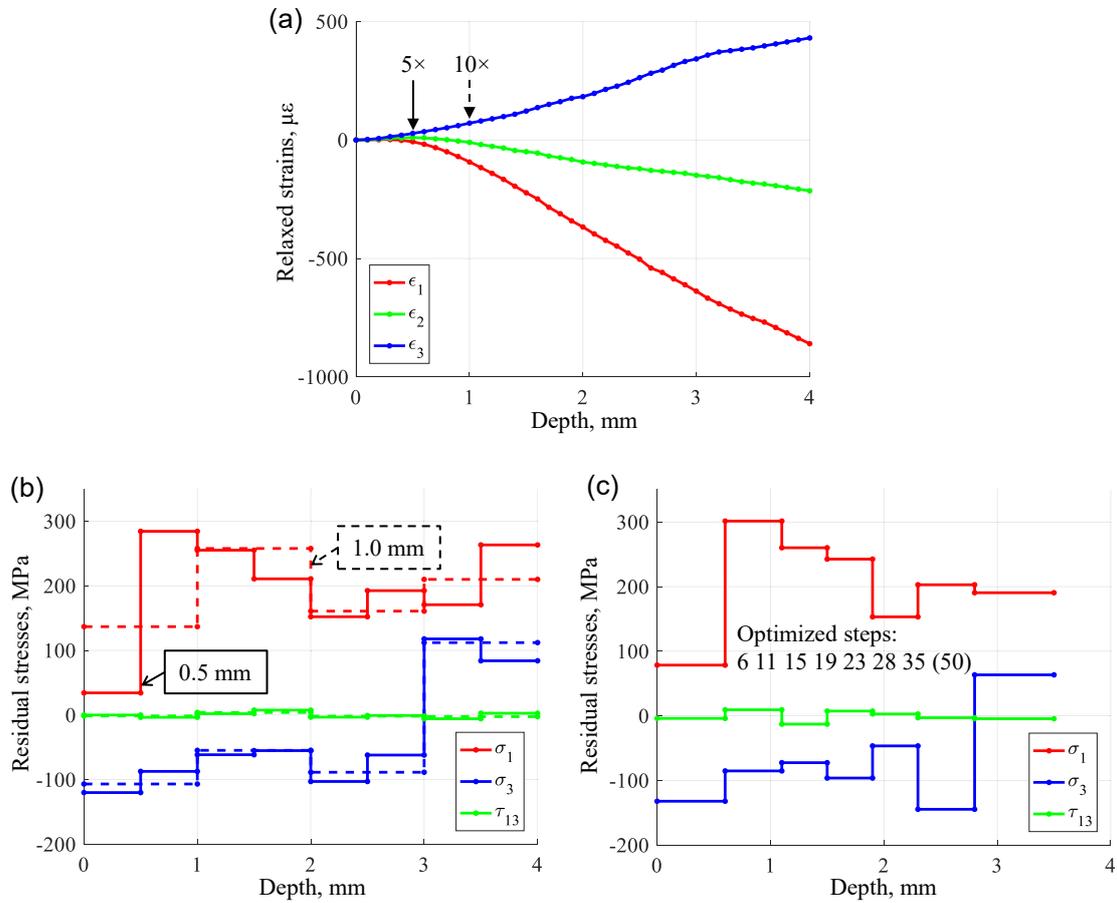
Figure 11. Ring-core experimental example, (a) relaxed strains with 0.1 mm incremental step, (b) residual stresses obtained with different depth steps: 0.5 mm and 1.0 mm, (c) residual stresses obtained with the optimized steps.

elements. In order to make the procedure suitable for processing experimentally obtained relaxed strains, a method for deriving lower resolution coefficients was proposed by which coarser and also non-uniform step sequences can be analysed. A more general form of the integral method, and the related coefficient analysis, confirmed that first order expansions of the relaxed strains, as a function of groove eccentricity with respect to the rosette centre, are zero. As a consequence, the integral method with the combined strains and stresses can be considered accurate enough even if the ring-core is produced with an eccentricity entity typical of the correct experimental implementation of the technique, hence still by using the proposed high resolution coefficient matrices. An example of practical application of the obtained coefficients was finally presented. The residual stress distributions obtained with different depth steps, and in particular with an optimized non-uniform step sequence, were calculated and compared, thus demonstrating the applicability of the lower resolution coefficient determination procedure.

Acknowledgements

References

1. ASTM E837 – 13a. Standard Test Method for Determining Residual Stresses by the Hole-Drilling Strain-Gage Method, 2013.

2. P.V. Grant, J.D. Lord, and P.S. Whitehead. Standard Test Method for Determining Residual Stresses by the Hole-Drilling Strain-Gage Method, 2002. National Physical Laboratory, Measurement Good Practice Guide No. 53, ISSN 1368-6550.

3. E. Procter and E.M. Beaney. Trepan or Ring Core Method, Centre-Hole Method, Sach's Method, Blind Hole Methods, Deep Hole Technique. *Advances in Surface Treatments*, 4:165–198, 1987.

4. W. Böhm, E. Stücker, and H. Wolf. Principles and potential applications of the ring-core method for determining residual stresses. *RAM*, 4:5–10, 1988.

5. A. Ajovalasit, G. Petrucci, and B. Zuccarello. Determination of nonuniform residual stresses using the ring-core method. *Journal of Engineering Materials and Technology, Transactions of the ASME*, 118(2):224–228, 1996.

6. B. Zuccarello. Optimization of depth increment distribution in the ring-core method. *Journal of Strain Analysis for Engineering Design*, 31(4):251–258, 1996.

7. F. Menda, F. Trebuňa, and P. Šarga. Determination of the necessary geometric parameters of the specimen in Ring-Core method. *Applied Mechanics and Materials*, 486:90–95, 2014.

8. F. Menda, P. Šarga, and F. Trebuňa. Estimation of residual stress field uniformity when using the ring-core method. *Advanced Materials Research*, 996:325–330, 2014.

9. F. Menda, P. Šarga, T. Lipták, and F. Trebuňa. Analysis of the geometric shape of the cutter in Ring-Core measurement. *Procedia Engineering*, 96:289–293, 2014.

10. B. Zuccarello, F. Menda, and M. Scafidi. Error and uncertainty analysis of non-uniform residual stress evaluation by using the ring-core method. *Experimental Mechanics*, 56(9):1531–1546, 2016.

11. A.J.G. Lunt, E. Salvati, L. Ma, I.P. Dolbyna, T.K. Neo, and A.M. Korsunsky. Full in-plane strain tensor analysis using the microscale ring-core FIB milling and DIC approach. *Journal of the Mechanics and Physics of Solids*, 94:47–67, 2016.

12. E. Salvati, T. Sui, A.J.G. Lunt, and A.M. Korsunsky. The effect of eigenstrain induced by ion beam damage on the apparent strain relief in FIB-DIC residual stress evaluation. *Materials and Design*, 92:649–658, 2016.

13. M. Beghini, L. Bertini, and L.F. Mori. Evaluating non-uniform residual stress by the hole-drilling method with concentric and eccentric holes. Part I. Definition and validation of the influence functions. *Strain*, 46:324–336, 2010.

14. M. Beghini, L. Bertini, and L.F. Mori. Evaluating non-uniform residual stress by the hole-drilling method with concentric and eccentric holes. Part II: Application of the influence functions to the inverse problem. *Strain*, 46:337–346, 2010.

15. M. Beghini, L. Bertini, and C. Santus. A procedure for evaluating high residual stresses using the blind hole drilling method, including the effect of plasticity. *Journal of Strain Analysis for Engineering Design*, 45:301–318, 2010.

16. M. Beghini, C. Santus, E. Valentini, and A. Benincasa. Experimental verification of the hole drilling plasticity effect correction. *Materials Science Forum*, 681:151–158, 2011.

17. A. Nau and B. Scholtes. Evaluation of the High-Speed Drilling Technique for the Incremental Hole-Drilling Method. *Experimental Mechanics*, 53:531–542, 2013.

18. A. Nau, D. von Mirbach, and B. Scholtes. Improved Calibration Coefficients for the Hole-Drilling Method Considering the Influence of the Poisson Ratio. *Experimental Mechanics*, 53:1371–1381, 2013.

19. P. Šarga and F. Menda. Comparison of Ring-Core Method and Hole-drilling Method Used for Determining Residual Stresses. *American Journal of Mechanical Engineering*, 1(7):335–338, 2013.

20. J. Václavík, O. Weinberg, P. Bohdan, J. Jankovec, and S. Holý. Evaluation of Residual Stresses using Ring Core Method. In *EPJ Web of Conferences, ICEM 14 - 14th International Conference on Experimental Mechanics*, volume 6 of *44004*, pages 1–6, 2010.

21. A. Giri and M.M. Mahapatra. On the measurement of sub-surface residual stresses in SS 304L welds by dry ring core technique. *Measurement*, 106:152–160, 2017.

22. L. Xu, H. Zhao, H. Jing, and Y. Han. Finite element analysis of calibration coefficients for residual stress measurements by the ring core procedure. *Materialpruefung/Materials Testing*, 56(11-12):923–928, 2014.

23. A. Civín and M. Vlk. Ring-Core Residual Stress Measurement: Analysis of Calibration Coefficients for Incremental Strain Method. *Bulletin of Applied Mechanics*, 6:77–83, 2010.

24. A. Civín and M. Vlk. Determination of principal residual stresses' directions by incremental strain method. *Applied and Computational Mechanics*, 5:5–14, 2011.

25. M. Barsanti, M. Beghini, L. Bertini, B.D. Monelli, and C. Santus. First-order correction to counter the effect of eccentricity on the hole-drilling integral method with strain-gage rosettes. *Journal of Strain Analysis for Engineering Design*, 51(6):431–443, 2016.

26. G.S. Schajer. Measurement of non-uniform residual stresses using the hole-drilling method. Part I. Stress calculation procedures. *Journal of Engineering Materials and Technology, Transactions of the ASME*, 110:338–343, 1988.

27. G.S. Schajer. Measurement of non-uniform residual stresses using the hole-drilling method. Part II. Practical application of the integral method. *Journal of Engineering Materials and Technology, Transactions of the ASME*, 110:344–349, 1988.

28. M. Beghini, L. Bertini, C. Santus, A. Benincasa, L. Bertelli, and E. Valentini. Validazione sperimentale di una rosetta a 6 griglie per ridurre l'errore di eccentricità nella misura delle tensioni residue. In *XXXIX congresso AIAS*, 2010. AIAS 2010 - 067.

29. P. Iurea, C. Carausu, C. Tampu, B. Chirita, and V. Husanu. Residual stresses generated at roughing grinding and hard turning of raceways of bearing rings. *International Journal of Modern Manufacturing Technologies*, 8(2):19–24, 2016.

30. E. Valentini, A. Benincasa, and L. Bertelli. An automatic system for measuring residual stresses by the ring-core method. In *XL congresso AIAS*, 2011. AIAS 2011 - 145.

31. M. Barsanti, M. Beghini, C. Santus, A. Benincasa, and L. Bertelli. Integral method coefficients and regularization procedure for the ring-core residual stress measurement technique. In *9th European Conference on Residual Stresses*, 2014. ECRS9, paper 242.

Appendix I

Notation

$D_\mathrm{I}, D_\mathrm{E}$	Internal and external diameter of the ring-core groove.
$G_\mathrm{L}, G_\mathrm{W}$	Grid length and width of the strain gage rosette.
ΔH	Groove depth incremental step.
H	Groove depth at a specific drilling step.
H_max	Maximum groove depth.
n	Number of the step increments at the final depth.
$\sigma_\mathrm{max}, \sigma_\mathrm{min}$	Principal maximum and minimum residual stresses.
ϑ	Generic grid orientation with respect to the maximum principal stress direction.
ε_r	Relaxed strain measured by a generic grid.
A, B	General elastic constants relating the residual stresses to the relaxed strains.
$\sigma_1, \sigma_3, \tau_{13}$	Residual stress components according to the rosette reference frame.
$\varepsilon_1, \varepsilon_2, \varepsilon_3$	Relaxed strains measured by the 0-45-90 degrees grids.
P, Q, T	Equibiaxial and shear combined stresses.
p, q, t	Combined relaxed strains according to the P, Q, T stresses.
E, ν	Young's modulus and Poisson's ratio material properties.
a, b	Calibration coefficients relating the P, Q, T residual stresses to the p, q, t relaxed strains.
$\mathbf{P}, \mathbf{Q}, \mathbf{T}$	Vectors containing the combined stresses along the depth.
$\mathbf{p}, \mathbf{q}, \mathbf{t}$	Vectors containing the combined strains along the depth.
$\bar{\mathbf{a}}, \bar{\mathbf{b}}$	Calibration coefficient matrices.
a_{ij}, b_{ij}	Calibration coefficient elements.
$\hat{\mathbf{t}}, \hat{\mathbf{n}}$	Transverse and normal unit vectors along the directions of the grid.
m	Integer multiple for lower resolution calibration matrices.
σ_x, σ_y	Stress components introduced as input for the FE 3D model validation.
$\mathbf{S}$	Vectors containing the blocks of the three uncoupled residual stress components.
$\mathbf{e}$	Vectors containing the blocks of the three grid relaxed strains.
$\bar{\mathbf{A}}$	Calibration coefficient 3×3 block matrix.
i, j	Calibration matrix depth indices, $i = 1, \ldots, n$ and $j = 1, \ldots, i$.
h, k	Block indexes, for the matrix $\bar{\mathbf{A}}$, ranging from 1 to 3.
e_1, e_3	Eccentricity components along the grid directions 1 and 3.

Coefficients for D_I = 14 mm, D_E = 18 mm, G_L = 5.0 mm, G_W = 2.5 mm, maximum depth H_{max} = 5.0 mm and depth resolution ΔH = 0.1 mm

$a_{ij} \times 10^3$ $b_{ij} \times 10^3$

$$\overline{a} = \begin{bmatrix} a_1 & \\ a_2 & a_3 \end{bmatrix} \qquad \overline{b} = \begin{bmatrix} b_1 & \\ b_2 & b_3 \end{bmatrix}$$

a_1

```
3.8156
5.3290 4.5008
6.6653 6.0634 5.0409
7.9566 7.3646 6.6656 5.4703
9.1961 8.6183 7.9611 7.1576 5.8154
10.394 9.8140 9.1928 8.4579 7.5586 6.0912
11.549 10.967 10.356 9.6764 8.8658 7.8817 6.3073
12.661 12.075 11.470 10.814 10.074 9.1941 8.1358 6.4704
13.730 13.140 12.537 11.897 11.191 10.393 9.4507 8.3278 6.5856
14.754 14.160 13.558 12.927 12.245 11.490 10.639 9.6415 8.4633 6.6574
15.732 15.136 14.534 13.908 13.241 12.517 11.716 10.818 9.7722 8.5471 6.6895
16.665 16.066 15.463 14.841 14.185 13.482 12.717 11.874 10.934 9.8473 8.5765 6.6855
17.552 16.951 16.347 15.728 15.080 14.391 13.652 12.849 11.969 10.993 9.8715 8.5765 6.6486
18.392 17.790 17.186 16.568 15.926 15.249 14.528 13.755 12.918 12.005 10.998 9.8488 8.5299 6.5818
19.187 18.584 17.979 17.363 16.725 16.057 15.351 14.600 13.795 12.928 11.987 10.955 9.7833 8.4472 6.4882
19.936 19.332 18.728 18.113 17.479 16.818 16.123 15.389 14.609 13.776 12.884 11.919 10.866 9.6788 8.3319 6.3705
20.641 20.037 19.432 18.818 18.187 17.532 16.847 16.126 15.365 14.559 13.703 12.788 11.805 10.737 9.5391 8.1874 6.2315
21.302 20.698 20.094 19.481 18.853 18.202 17.525 16.815 16.070 15.285 14.456 13.579 12.647 11.649 10.571 9.3678 8.0168 6.0737
21.921 21.317 20.713 20.102 19.476 18.830 18.158 17.458 16.725 15.957 15.151 14.303 13.409 12.463 11.455 10.372 9.1683 7.8233 5.8996
22.498 21.895 21.292 20.682 20.058 19.415 18.750 18.057 17.335 16.581 15.793 14.968 14.104 13.197 12.242 11.228 10.143 8.9439 7.6097 5.7116
23.036 22.434 21.832 21.222 20.601 19.961 19.300 18.615 17.901 17.159 16.386 15.580 14.740 13.864 12.948 11.986 10.971 9.8890 8.6980 7.3790 5.5118
23.536 22.935 22.333 21.726 21.106 20.469 19.813 19.132 18.427 17.694 16.934 16.144 15.323 14.472 13.586 12.664 11.701 10.687 9.6123 8.4336 7.1337 5.3025
24.000 23.400 22.799 22.193 21.575 20.941 20.288 19.613 18.914 18.190 17.440 16.663 15.859 15.027 14.166 13.275 12.351 11.389 10.381 9.3162 8.1535 6.8763 5.0855
24.428 23.830 23.230 22.625 22.009 21.378 20.728 20.057 19.364 18.648 17.907 17.141 16.351 15.535 14.695 13.828 12.935 12.012 11.055 10.056 9.0041 7.8605 6.6093 4.8626
24.824 24.227 23.629 23.025 22.410 21.782 21.135 20.468 19.780 19.070 18.337 17.581 16.802 16.001 15.177 14.331 13.462 12.569 11.650 10.701 9.7138 8.6786 7.5571 6.3349 4.6356
```

a_2

```
25.189 24.593 23.996 23.393 22.781 22.154 21.510 20.847 20.164 19.459 18.733 17.985 17.216 16.427 15.617 14.788 13.939 13.071 12.181 11.270 10.331 9.3587 8.3426 7.2459 6.0550
25.524 24.929 24.333 23.733 23.122 22.497 21.856 21.196 20.516 19.817 19.096 18.356 17.596 16.816 16.019 15.204 14.372 13.523 12.658 11.775 10.873 9.9484 8.9932 7.9987 6.9289
25.832 25.238 24.644 24.044 23.435 22.812 22.173 21.516 20.840 20.145 19.430 18.696 17.943 17.173 16.385 15.582 14.765 13.933 13.087 12.228 11.355 10.465 9.5557 8.6200 7.6490
26.113 25.520 24.928 24.329 23.722 23.101 22.464 21.810 21.137 20.446 19.736 19.007 18.261 17.498 16.720 15.927 15.121 14.303 13.475 12.634 11.784 10.922 10.047 9.1555 8.2414
26.370 25.779 25.187 24.590 23.984 23.365 22.730 22.079 21.409 20.721 20.015 19.292 18.551 17.795 17.024 16.241 15.445 14.639 13.824 13.000 12.168 11.328 10.480 9.6217 8.7505
26.604 26.014 25.424 24.828 24.224 23.606 22.973 22.324 21.657 20.973 20.270 19.551 18.816 18.066 17.302 16.526 15.739 14.943 14.139 13.329 12.512 11.691 10.864 10.032 9.1925
26.817 26.229 25.640 25.045 24.442 23.826 23.195 22.548 21.884 21.202 20.503 19.788 19.057 18.312 17.554 16.784 16.005 15.218 14.424 13.625 12.822 12.016 11.206 10.395 9.5804
27.010 26.423 25.835 25.242 24.640 24.026 23.397 22.751 22.089 21.410 20.714 20.002 19.276 18.535 17.782 17.019 16.247 15.467 14.682 13.892 13.100 12.306 11.512 10.717 9.9228
27.186 26.599 26.013 25.421 24.820 24.207 23.579 22.936 22.276 21.599 20.906 20.198 19.474 18.738 17.990 17.232 16.466 15.692 14.914 14.133 13.350 12.567 11.785 11.005 10.226
27.344 26.759 26.173 25.583 24.983 24.371 23.745 23.103 22.445 21.771 21.080 20.374 19.654 18.921 18.177 17.424 16.662 15.895 15.124 14.350 13.575 12.801 12.029 11.261 10.496
27.486 26.903 26.318 25.728 25.130 24.519 23.895 23.254 22.598 21.925 21.237 20.534 19.817 19.087 18.347 17.597 16.840 16.078 15.312 14.545 13.777 13.011 12.248 11.489 10.735
27.615 27.032 26.448 25.860 25.262 24.653 24.029 23.391 22.736 22.065 21.379 20.678 19.963 19.236 18.499 17.753 17.001 16.243 15.482 14.720 13.958 13.199 12.443 11.693 10.949
27.730 27.148 26.565 25.978 25.381 24.773 24.151 23.513 22.860 22.191 21.506 20.807 20.095 19.371 18.637 17.894 17.145 16.391 15.634 14.877 14.121 13.367 12.618 11.875 11.138
27.833 27.252 26.670 26.083 25.488 24.881 24.259 23.623 22.971 22.303 21.621 20.923 20.213 19.491 18.760 18.020 17.274 16.523 15.771 15.018 14.266 13.518 12.774 12.037 11.307
27.924 27.344 26.764 26.178 25.583 24.977 24.357 23.721 23.071 22.404 21.723 21.028 20.319 19.599 18.870 18.133 17.389 16.642 15.893 15.143 14.396 13.652 12.913 12.181 11.458
28.006 27.427 26.847 26.262 25.668 25.062 24.443 23.809 23.159 22.494 21.814 21.120 20.414 19.696 18.969 18.233 17.493 16.748 16.002 15.255 14.511 13.771 13.037 12.310 11.591
28.079 27.500 26.921 26.336 25.743 25.139 24.520 23.887 23.238 22.574 21.896 21.203 20.498 19.782 19.056 18.323 17.584 16.842 16.098 15.355 14.614 13.878 13.147 12.424 11.710
28.143 27.565 26.986 26.403 25.810 25.206 24.588 23.956 23.309 22.646 21.969 21.277 20.573 19.858 19.134 18.403 17.666 16.926 16.185 15.444 14.706 13.972 13.244 12.525 11.814
28.199 27.622 27.044 26.461 25.869 25.266 24.649 24.017 23.370 22.708 22.032 21.341 20.639 19.925 19.203 18.473 17.738 17.000 16.261 15.522 14.786 14.055 13.330 12.614 11.907
28.248 27.672 27.094 26.512 25.921 25.318 24.702 24.071 23.425 22.764 22.089 21.397 20.697 19.985 19.264 18.535 17.802 17.065 16.327 15.591 14.857 14.129 13.406 12.692 11.988
28.292 27.715 27.139 26.557 25.966 25.364 24.748 24.118 23.472 22.812 22.137 21.449 20.748 20.037 19.317 18.590 17.858 17.123 16.387 15.652 14.920 14.193 13.473 12.762 12.060
28.329 27.753 27.177 26.595 26.005 25.404 24.788 24.159 23.513 22.854 22.180 21.492 20.793 20.083 19.364 18.638 17.907 17.173 16.438 15.705 14.975 14.253 13.531 12.822 12.123
28.361 27.786 27.210 26.629 26.039 25.438 24.823 24.194 23.550 22.891 22.217 21.530 20.832 20.122 19.404 18.679 17.949 17.217 16.483 15.751 15.022 14.299 13.582 12.875 12.177
28.389 27.814 27.239 26.658 26.069 25.468 24.853 24.225 23.581 22.922 22.249 21.563 20.865 20.156 19.439 18.715 17.986 17.254 16.522 15.791 15.064 14.342 13.627 12.920 12.224
28.413 27.838 27.263 26.683 26.093 25.493 24.879 24.251 23.607 22.949 22.277 21.591 20.894 20.186 19.469 18.746 18.018 17.287 16.556 15.826 15.099 14.378 13.665 12.960 12.265
```

a_3

```
4.4061
5.7715 4.1753
6.6083 5.4863 3.9446
7.2959 6.2859 5.2007 3.7152
7.8597 6.9413 5.9634 4.9164 3.4881
8.3429 7.4769 6.5870 5.6424 4.6344 3.2642
8.7613 7.9348 7.0950 6.2346 5.3243 4.3560 3.0442
9.1276 8.3302 7.5282 6.7156 5.8857 5.0102 4.0821 2.8290
9.4500 8.6755 7.9012 7.1246 6.3402 5.5414 4.7014 3.8137 2.6191
9.7349 8.9786 8.2261 7.4760 6.7258 5.9701 5.2030 4.3986 3.5514 2.4149
9.9874 9.2459 8.5107 7.7813 7.0561 6.3329 5.6066 4.8714 4.1028 3.2959 2.2170
10.211 9.4821 8.7610 8.0480 7.3424 6.6430 5.9473 5.2507 4.5475 3.8146 3.0478 2.0257
10.410 9.6913 8.9817 8.2803 7.5919 6.9110 6.2377 5.5347 4.9150 4.2341 3.5347 2.8074 1.8412
10.587 9.8765 9.1765 8.4878 7.8103 7.1440 6.4881 5.8415 5.2018 4.5649 3.9257 3.2634 2.5751 1.6637
10.744 10.041 9.3487 8.6690 8.0018 7.3473 6.7052 6.0749 5.4551 4.8436 4.2364 3.6288 3.0013 2.3513 1.4934
10.883 10.186 9.5008 8.8287 8.1701 7.5252 6.8943 6.2768 5.6722 5.0793 4.4959 3.9182 3.3420 2.7485 2.1361 1.3303
11.006 10.314 9.6350 8.9694 8.3179 7.6811 7.0592 6.4521 5.8595 5.2809 4.7147 4.1593 3.6109 3.0654 2.5054 1.9295 1.1746
11.115 10.428 9.7535 9.0932 8.4478 7.8177 7.2024 6.6046 6.0217 5.4542 4.9014 4.3620 3.8342 3.3145 2.7993 2.2720 1.7319 1.0262
11.211 10.528 9.8577 9.2022 8.5618 7.9373 7.3291 6.7374 6.1624 5.6038 5.0614 4.5343 4.0213 3.5208 3.0295 2.5438 2.0484 1.5430 0.88503
11.296 10.616 9.9493 9.2977 8.6617 8.0419 7.4389 6.8531 6.2845 5.7332 5.1990 4.6815 4.1799 3.6932 3.2195 2.7593 2.2991 1.8408 1.3629 0.75111
11.370 10.693 10.030 9.3814 8.7491 8.1334 7.5348 6.9537 6.3905 5.8451 5.3177 4.8078 4.3151 3.8387 3.3777 2.9304 2.4938 2.0652 1.6310 1.1917 0.62427
11.435 10.760 10.100 9.4545 8.8254 8.2130 7.6171 7.0411 6.4825 5.9419 5.4200 4.9162 4.4305 3.9623 3.5108 3.0750 2.6534 2.2433 1.8420 1.4369 1.0290 0.50445
11.492 10.820 10.161 9.5133 8.8917 8.2823 7.6905 7.1169 6.5619 6.0256 5.5081 5.0094 4.5292 4.0674 3.6233 3.1962 2.7867 2.3887 2.0042 1.6294 1.2526 0.87490 0.39144
11.541 10.870 10.214 9.5733 8.9491 8.3422 7.7531 7.1824 6.6305 6.0976 5.5838 5.0892 4.6137 4.1569 3.7186 3.2983 2.8951 2.5082 2.1361 1.7766 1.4274 1.0777 0.72920 0.28509
11.583 10.914 10.260 9.6209 8.9987 8.3939 7.8071 7.2388 6.6895 6.1595 5.6488 5.1576 4.6857 4.2331 3.7994 3.3843 2.9872 2.6074 2.2439 1.8956 1.5602 1.2357 0.91223 0.59162 0.18524
```

b_1

```
5.2582
6.7987 5.9027
8.2099 7.5041 6.4355
9.6160 8.8915 8.1143 6.8750
11.007 10.277 9.5120 8.6368 7.2450
12.396 11.644 10.894 10.059 9.0867 7.5592
13.784 13.009 12.248 11.449 10.538 9.4742 7.8252
15.171 14.373 13.597 12.799 11.941 10.954 9.8063 8.0481
16.558 15.736 14.940 14.137 13.291 12.370 11.312 10.087 8.2314
17.944 17.097 16.280 15.464 14.621 13.722 12.741 11.616 10.321 8.3776
19.327 18.456 17.617 16.785 15.935 15.046 14.093 13.054 11.868 10.509 8.4888
20.706 19.810 18.948 18.098 17.237 16.347 15.411 14.407 13.313 12.071 10.655 8.5666
22.078 21.158 20.273 19.403 18.528 17.632 16.700 15.717 14.663 13.520 12.226 10.760 8.6126
23.443 22.499 21.590 20.699 19.807 18.901 17.967 16.992 15.964 14.865 13.675 12.336 10.826 8.6285
24.799 23.830 22.897 21.984 21.074 20.155 19.213 18.240 17.224 16.154 15.012 13.782 12.403 10.854 8.6157
26.142 25.148 24.192 23.256 22.327 21.393 20.441 19.464 18.453 17.398 16.288 15.109 13.842 12.428 10.847 8.5758
27.471 26.453 25.473 24.515 23.566 22.614 21.651 20.666 19.654 18.606 17.514 16.369 15.155 13.857 12.413 10.807 8.5104
28.785 27.742 26.738 25.757 24.788 23.818 22.840 21.846 20.828 19.781 18.699 17.574 16.397 15.154 13.829 12.361 10.735 8.4210
30.080 29.013 27.985 26.981 25.991 25.003 24.010 23.003 21.978 20.928 19.849 18.736 17.581 16.376 15.108 13.761 12.274 10.633 8.3094
31.356 30.264 29.212 28.186 27.175 26.168 25.158 24.138 23.102 22.047 20.968 19.859 18.718 17.537 16.309 15.020 13.654 12.154 10.504 8.1771
32.610 31.494 30.418 29.370 28.337 27.311 26.284 25.249 24.202 23.139 22.055 20.948 19.813 18.647 17.444 16.196 14.891 13.512 12.003 10.349 8.0259
33.840 32.700 31.601 30.530 29.476 28.431 27.386 26.336 25.277 24.203 23.114 22.004 20.872 19.714 18.527 17.305 16.042 14.724 13.338 11.824 10.170 7.8575
35.046 33.882 32.760 31.667 30.592 29.527 28.464 27.398 26.321 25.241 24.143 23.028 21.895 20.741 19.564 18.359 17.123 15.849 14.523 13.132 11.619 9.9701 7.6736
36.226 35.038 33.893 32.778 31.682 30.597 29.516 28.435 27.347 26.251 25.144 24.023 22.886 21.733 20.560 19.366 18.148 16.902 15.620 14.290 12.899 11.390 9.7507 7.4757
37.378 36.167 34.999 33.862 32.745 31.641 30.543 29.444 28.343 27.234 26.116 24.987 23.845 22.689 21.519 20.331 19.125 17.897 16.643 15.358 14.028 12.640 11.139 9.5140 7.2656
```

b_2

```
38.501 37.267 36.077 34.919 33.782 32.658 31.542 30.427 29.310 28.189 27.060 25.921 24.773 23.613 22.441 21.256 20.057 18.842 17.608 16.351 15.065 13.739 12.359 10.870 9.9620
39.595 38.338 37.136 35.947 34.790 33.647 32.513 31.382 30.250 29.115 27.974 26.826 25.670 24.505 23.330 22.146 20.950 19.742 18.521 17.285 16.028 14.746 13.426 12.057 10.583
40.659 39.379 38.146 36.946 35.769 34.608 33.456 32.309 31.162 30.013 28.861 27.702 26.538 25.366 24.187 23.000 21.805 20.602 19.390 18.167 16.930 15.678 14.402 13.093 11.737
41.691 40.390 39.136 37.915 36.719 35.540 34.370 33.207 32.045 30.883 29.718 28.549 27.375 26.196 25.011 23.821 22.626 21.424 20.217 19.003 17.781 16.549 15.303 14.037 12.741
42.692 41.370 40.095 38.854 37.639 36.442 35.256 34.076 32.900 31.724 30.546 29.367 28.183 26.996 25.805 24.611 23.412 22.211 21.006 19.798 18.585 17.368 16.142 14.906 13.653
43.661 42.318 41.023 39.762 38.529 37.311 36.112 34.916 33.725 32.536 31.346 30.155 28.962 27.767 26.569 25.369 24.167 22.964 21.760 20.555 19.349 18.141 16.930 15.715 14.491
44.598 43.234 41.919 40.641 39.390 38.157 36.938 35.728 34.522 33.319 32.118 30.915 29.712 28.508 27.303 26.097 24.891 23.685 22.480 21.276 20.074 18.872 17.672 16.472 15.269
45.503 44.119 42.785 41.488 40.219 38.970 37.735 36.510 35.290 34.074 32.860 31.647 30.434 29.221 28.008 26.796 25.585 24.375 23.168 21.964 20.763 19.566 18.373 17.183 15.995
46.375 44.972 43.620 42.305 41.019 39.754 38.503 37.263 36.030 34.801 33.575 32.351 31.128 29.906 28.685 27.466 26.249 25.036 23.826 22.620 21.420 20.227 19.037 17.854 16.676
47.216 45.794 44.423 43.091 41.789 40.507 39.242 37.987 36.741 35.500 34.262 33.027 31.794 30.563 29.335 28.109 26.886 25.667 24.452 23.246 22.045 20.851 19.665 18.488 17.318
48.024 46.584 45.196 43.847 42.528 41.232 39.952 38.684 37.424 36.171 34.922 33.676 32.433 31.194 29.957 28.724 27.495 26.271 25.054 23.843 22.641 21.447 20.262 19.087 17.922
48.801 47.343 45.938 44.573 43.239 41.928 40.633 39.352 38.080 36.814 35.554 34.298 33.046 31.797 30.553 29.312 28.077 26.849 25.627 24.413 23.208 22.013 20.828 19.655 18.494
49.547 48.072 46.650 45.270 43.921 42.595 41.287 39.992 38.708 37.431 36.160 34.894 33.632 32.375 31.123 29.875 28.634 27.400 26.173 24.955 23.748 22.551 21.366 20.193 19.034
50.262 48.770 47.330 45.938 44.574 43.234 41.913 40.606 39.310 38.021 36.740 35.466 34.197 32.933 31.674 30.421 29.172 27.930 26.694 25.473 24.262 23.063 21.876 20.704 19.545
50.947 49.439 47.987 46.577 45.199 43.846 42.512 41.193 39.885 38.586 37.295 36.009 34.730 33.456 32.188 30.927 29.673 28.427 27.191 25.965 24.751 23.549 22.361 21.188 20.029
51.603 50.079 48.612 47.188 45.797 44.431 43.085 41.754 40.435 39.126 37.824 36.530 35.240 33.957 32.684 31.416 30.160 28.910 27.664 26.424 25.192 23.967 22.782 21.611 20.457
52.229 50.691 49.210 47.772 46.368 44.990 43.632 42.290 40.960 39.641 38.330 37.027 35.730 34.440 33.158 31.883 30.617 29.361 28.115 26.880 25.659 24.451 23.258 22.082 20.922
52.828 51.273 49.781 48.330 46.913 45.523 44.154 42.801 41.462 40.132 38.812 37.500 36.196 34.899 33.609 32.328 31.056 29.794 28.543 27.304 26.079 24.868 23.673 22.495 21.334
53.399 51.833 50.325 48.862 47.433 46.032 44.652 43.289 41.939 40.601 39.272 37.951 36.639 35.335 34.038 32.751 31.473 30.206 28.950 27.707 26.478 25.264 24.066 22.886 21.723
53.944 52.367 50.844 49.369 47.929 46.516 45.126 43.753 42.394 41.046 39.709 38.381 37.061 35.749 34.447 33.154 31.870 30.597 29.337 28.090 26.857 25.640 24.439 23.256 22.092
54.462 52.871 51.338 49.851 48.400 46.977 45.577 44.194 42.826 41.470 40.125 38.789 37.462 36.144 34.835 33.536 32.247 30.970 29.705 28.454 27.217 25.996 24.793 23.607 22.441
54.956 53.382 51.808 50.310 48.849 47.416 46.006 44.614 43.238 41.874 40.520 39.177 37.843 36.519 35.204 33.899 32.605 31.323 30.054 28.799 27.558 26.334 25.128 23.940 22.771
55.426 53.810 52.250 50.747 49.275 47.833 46.414 45.013 43.628 42.257 40.896 39.546 38.205 36.874 35.554 34.243 32.944 31.658 30.384 29.125 27.881 26.654 25.445 24.255 23.084
55.872 54.246 52.680 51.162 49.680 48.229 46.801 45.392 43.999 42.620 41.252 39.895 38.549 37.212 35.886 34.570 33.266 31.975 30.697 29.434 28.187 26.957 25.745 24.552 23.379
56.296 54.659 53.083 51.555 50.065 48.604 47.168 45.751 44.351 42.965 41.590 40.227 38.874 37.532 36.200 34.880 33.571 32.276 30.994 29.727 28.477 27.244 26.029 24.834 23.659
```

b_3

```
7.0449
8.9966 6.8150
10.282 8.7196 6.5774
11.402 9.9687 8.4330 6.3336
12.373 11.054 9.6445 8.1384 6.0849
13.254 11.992 10.695 9.3117 7.8374 5.8326
14.060 12.840 11.600 10.326 8.9720 7.5317 5.5777
14.807 13.616 12.416 11.198 9.9512 8.6273 7.2226 5.3216
15.503 14.333 13.161 11.983 10.793 9.5789 8.2790 6.9116 5.0651
16.155 14.999 13.848 12.698 11.544 10.377 9.1872 7.9288 6.5998 4.8092
16.768 15.623 14.486 13.356 12.229 11.100 9.9632 8.8017 7.5779 6.2884 4.5547
17.344 16.207 15.081 13.965 12.858 11.755 10.654 9.5437 8.4159 7.2277 5.9785 4.3026
17.888 16.757 15.638 14.533 13.440 12.357 11.280 10.206 9.1264 8.0312 6.8794 5.6710 4.0534
18.402 17.274 16.161 15.064 13.981 12.912 11.854 10.805 9.7599 8.7107 7.6487 6.5338 5.3669 3.8078
18.887 17.762 16.653 15.561 14.486 13.427 12.383 11.352 10.331 9.3155 8.2979 7.2697 6.1922 5.0668 3.5664
19.346 18.222 17.116 16.029 14.959 13.908 12.873 11.855 10.852 9.8595 8.8747 7.8890 6.8955 5.8343 4.7715 3.3296
19.780 18.657 17.553 16.468 15.402 14.357 13.330 12.322 11.331 10.355 9.3925 8.4384 7.4854 6.5258 5.5236 4.4816 3.0980
20.191 19.068 17.964 16.881 15.819 14.781 13.756 12.755 11.771 10.811 9.8640 8.9311 8.0087 7.0677 6.1627 5.1981 4.1977 2.8717
20.580 19.456 18.353 17.271 16.210 15.172 14.155 13.159 12.185 11.231 10.296 9.3787 8.4762 7.5845 6.6969 5.8064 4.8794 3.9201 2.6514
20.947 19.823 18.719 17.638 16.579 15.542 14.538 13.537 12.568 11.621 10.695 9.7886 8.9009 8.0280 7.1685 6.3136 5.4575 4.5678 3.6493 2.4370
21.295 20.169 19.066 17.984 16.926 15.890 14.878 13.890 12.925 11.983 11.064 10.166 9.2891 8.4312 7.5895 6.7609 5.9386 5.1166 4.2693 3.3856 2.2289
21.623 20.497 19.392 18.311 17.252 16.218 15.207 14.221 13.259 12.321 11.406 10.515 9.6469 8.7987 7.9705 7.1594 6.3621 5.5723 4.7893 3.9679 3.1294 2.0273
21.934 20.806 19.701 18.619 17.560 16.526 15.516 14.531 13.571 12.636 11.725 10.839 9.9763 9.1364 8.3181 7.5198 6.7391 5.9729 5.2151 4.4605 3.6802 2.8808 1.8323
22.228 21.099 19.992 18.909 17.850 16.816 15.807 14.823 13.864 12.931 12.023 11.140 10.282 9.4481 8.6370 7.8481 7.0794 6.3290 5.5936 4.8676 4.1459 3.4011 2.6399 1.6439
22.505 21.375 20.267 19.183 18.123 17.089 16.080 15.096 14.139 13.207 12.301 11.421 10.566 9.7366 8.9311 8.1490 7.3891 6.6501 5.9295 5.2246 4.5300 3.8407 3.1306 2.4070 1.4623
```